Subterranean Biology 52: 143–186 (2025)
https://doi.org/10.3897/subtbiol.52.142334
https://subtbiol.pensoft.net

RESEARCH ARTICLE

A peer-reviewed open-access journal
Subterranean Biology
Published by The International Society for Subterranean Biology

Revisiting and rediscovering the tarantulas (Araneae, Theraphosidae) of Culapnitan (Libmanan) Caves in the Philippines: troglomorphism, taxonomy, phylogeny and ecological niche

Darrell C. Acuña[1,2,3], Lorenz Rhuel P. Ragasa[1], Myla R. Santiago-Bautista[1,4], Volker von Wirth[5], Leonardo A. Guevarra Jr.[1,2,4]

1 *Research Center for Natural and Applied Sciences, University of Santo Tomas, España Blvd., Sampaloc, Manila 1008, Philippines* **2** *Philippine Arachnological Society, Inc., Paco, Manila 1007, Philippines* **3** *Graduate School, Polytechnic University of the Philippines, Sta. Mesa, Manila 1016, Philippines* **4** *Department of Biochemistry, Faculty of Pharmacy, University of Santo Tomas, España Blvd., Sampaloc, Manila 1008, Philippines* **5** *Theraphosid Research Team, Hofmarkstr. 6, Eitting 85462, Germany*

Corresponding author: Leonardo A. Guevarra Jr. (laguevarra@ust.edu.ph)

Academic editor: Giuseppe Nicolosi | Received 21 November 2024 | Accepted 28 January 2025 | Published 5 June 2025

https://zoobank.org/C990F793-3677-4A43-AE8E-F8CB7552B138

Citation: Acuña DC, Ragasa LRP, Santiago-Bautista MR, von Wirth V, Guevarra Jr LA (2025) Revisiting and rediscovering the tarantulas (Araneae, Theraphosidae) of Culapnitan (Libmanan) Caves in the Philippines: troglomorphism, taxonomy, phylogeny and ecological niche. Subterranean Biology 52: 143–186. https://doi.org/10.3897/subtbiol.52.142334

Abstract

In 1892, French naturalist Eugène Simon described samples of cave-dwelling tarantula species collected from Culapnitan Caves in the Philippines, a cave system that is now part of the present-time Libmanan Caves Natural Park (LCNP). One of these is the new monotypic tarantula genus and species of that time, *Orphnaecus pellitus* Simon, 1892. Based on Simon's notes and quick observation of the eyes of the syntypes, this species is highly suspected to be troglobitic. In the present study, we rediscovered *O. pellitus* from its reported site and investigated its troglobitic characteristics. Morphological analysis of *O. pellitus* shows troglomorphic characteristics which include reduced eye size, attenuated limbs, shortened tactile setae, and diminishing pigmentation. Tolerance to hypoxia and heightened sensitivity to ground movements are the other subterranean adaptations that were observed. Phylogenetic analysis revealed a cladistic relationship among tarantula morphologically identified from the genus *Orphnaecus*. Our findings provide evidence that *O. pellitus* is a true troglobitic tarantula reported worldwide, and currently the only one known from Asia. We also report two new species of *Orphnaecus*, *Orphnaecus libmanan* **sp. nov.** and the dwarf *Orphnaecus tangcongvaca* **sp. nov.**, collected from the forest grounds of the LCNP. The ecological niche differentiation of theraphosid species in the LCNP is also provided. Our findings are supported by morphology, molecular phylogeny, and ecology.

Copyright *Darrell C. Acuña et al.* This is an open access article distributed under the terms of the Creative Commons Attribution License (CC BY 4.0), which permits unrestricted use, distribution, and reproduction in any medium, provided the original author and source are credited.

Keywords
Cave spiders, dwarf tarantula, niche partitioning, *Orphnaecus*, Philippine tarantula, Selenocosmiinae, spider ecology, troglobiont, troglomorphism

Introduction

Karsts are considered arks of biodiversity because of the high endemism of living organisms found on different karst structures. Some of the fascinating structures created in karst formations are caves (Clements et al. 2006). These fascinating ecosystems are characterised by darkness, temperature stability, relative humidity, and limited access to nutrients and energy sources (Trajano 2012).

Caves are considered natural laboratories owing to the simplicity of their ecosystem. Thus, studying cave fauna can help us understand evolutionary processes (Poulson and White 1969; Juan et al. 2010). Caves often harbour unique and specialised species adapted to subterranean environments. Some of these are troglobitic species which generally exhibit troglomorphism or evolutionary adaptation to cave ecosystems (Behrmann-Godel et al. 2017).

The total coverage area of karsts in Southeast Asia is approximately 400,000 km^2, 35,000 km^2 of which is in the Philippines (Clements et. al 2006; Restificar et al. 2006). Most caves in the Philippines are predominantly composed of limestone formations which, by nature, are moist and hence a suitable environment for many living organisms (Palmer 1991; Restificar et al. 2006). The caves in the Philippines are known to be the type locality of notable troglobitic arthropod species which include the freshwater crab *Sundathelphusa waray* Husana et al., 2009, the noctiolid cockroach *Nocticola gonzalezi* Lucañas & Lit, 2016, and the chaerilid scorpion *Chaerilus agnellivanniorum* Lourenco & Rossi, 2018. Similar to these Philippine troglobitic species, many other troglobitic species are often found limitedly in one cave system and cannot be found elsewhere (Vandel 1965; Stoch 2002; Culver and Pipan 2009; Deharveng and Bedos 2012).

Troglobitic species are obligate dwellers of cave environments (Culver and Pipan 2009). Since they spend their whole life cycle exclusively inside the caves, troglobites were able to develop certain morphological, physiological, and behavioural characteristics to adapt to life in subterranean habitats (Howarth 1983; Gibert and Deharveng 2002; Culver and Pipan 2009; Romero 2009; de Souza et al. 2024).

One group of arthropods that can colonise cave ecosystems are spiders (Mammola and Isaia 2017). Spiders, such as those from the family Theraphosidae, were able to adapt to cave ecosystems and developed troglobitic characters. There are at least 18 recognised true troglobitic tarantula species from three genera of tarantula worldwide (Bertani et al. 2013; Bloom et al. 2014; Mendoza 2014; Mendoza and Francke 2018). All these species are from the Neotropics (specifically from Mexico, Dominican Republic, and Brazil), with Mexico holding the most diversity due to

its extensive cave systems (Mendoza and Francke 2018). These tarantulas which express varying degrees of troglomorphism are from three genera—*Hemirrhagus* Simon, 1903 (16 species), *Holothele* Karsch, 1879 (1 species), and *Tmesiphantes* Simon, 1892 (1 species), wherein the observed troglomorphic traits from the different species include reduction or absence of eyes, elongation and attenuation of legs, and diminishing of pigmentation (Bertani et al. 2013; Bloom et al. 2014; Mendoza 2014; Mendoza and Francke 2018).

In contrast to South America, there is no recognised troglobitic tarantula in Asia. The presence of two Philippine cave-dwelling tarantulas discovered more than a century apart has been reported (Simon 1892; Barrion-Dupo et al. 2015). The first cave-dwelling tarantula, *Orphnaecus pellitus* Simon, 1892, was reported in 1892 by Eugène Simon and was collected from "Calapnitan Caves" [Culapnitan Caves], a cave system that is now part of the Libmanan Caves National Park (LCNP), Camarines Sur in, Luzon Island. The second, *Orphnaecus kwebaburdeos* (Barrion-Dupo et al., 2015), was collected from the Puting Bato Caves, Polillo Island, an island off the coast of the main island of Luzon in Quezon Province. Although both were cave-dwelling, none of them were classified as troglobitic species. *O. kwebaburdeos* is reported to be spending its whole life cycle inside the cave but does not exhibit troglomorphism (Barrion-Dupo et al. 2015). In contrast, Simon (1892) described *O. pellitus* as having tiny and more separated eyes, which, as he explained, may be a consequence of living inside the cave but is still unrecognised as a troglobitic tarantula due to its poorly known biology (Simon 1892).

In this study, we revisited Culapnitan Caves in the LCNP, the type locality of *O. pellitus*, to collect and reinvestigate the morphological features and observe the biology of this possibly troglobitic tarantula species using newly collected specimens. We also collected and described tarantula species from outside the caves which are part of the LCNP and adjacent areas surrounding these currently protected cave systems.

Material and methods

Specimen collection

A gratuitous permit was acquired from the Philippines' Department of Environment and Natural Resources-Biodiversity Management Bureau (DENR-BMB), as well as consent from the Protected Areas Management Bureau-Libmanan Caves National Park (PAMB-LCNP) and the local government of the Municipality of Libmanan. Specimens were manually collected from mid-day to night and preserved in 80% ethanol. Location coordinates (GPS) are omitted due to the risk of illegal wildlife trafficking as suggested by Lindenmayer and Sheele (2017) and Midgeley and Engelbrecht (2019). GPS coordinates, however, are available for specimens which are temporarily stored at the Arachnid Reference Collection (ARC) of the Research Center for Natural and Applied Sciences, University of Santo Tomas for viewing and reference purposes.

Species concept

The species concept used in this study was based on the Unified Species Concept proposed by de Queiroz (2005, 2007). A combination of evidence was employed to identify independently evolving lineages.

Morphological analysis

The morphological descriptive format mostly followed Acuña et al. (2025) which includes the description and terminologies for the setation and palpal organ structures, and morphometric indices (as provided below). The current taxonomy and diagnosis of *Orphnaecus* followed the revision of Acuña et al. (2025) (*Selenobrachys* Schmidt, 1999 and *Chilocosmia* Schmidt & von Wirth, 1992 were removed from synonymy with *Orphnaecus*). Morphological examination of the type specimens of different Selenocosmiinae species was performed by personal examination at the University of the Philippines Los Baños-Museum of Natural History (UPLB-MNH), Laguna, the National Museum of the Philippines (PNM), Manila, and the Muséum National d'Histoire Naturelle (MNHN), Paris. The allotype/paratype female (PNM 14888) of *O. adamsoni* was excluded from the analysis because the specimen does not belong to *Orphnaecus* based on its characteristics that do not fit in the synapomorphy of Selenocosmiinae, but in Ornithoctoninae (see explanation in the Results).

The materials of the subject species described in this study are listed on their respective taxonomic treatments. The other selenocosmiine comparative materials (types and non-types) examined and used in this study are: *Orphnaecus adamsoni* Salamanes et. al., 2022: Philippines: Dinagat Is.—Dinagat Islands Prov. ***holotype*** • ♂ PNM 14889; Loreto, Mt. Mangkuno; Oct 2018, J Santos & GG Villancio leg., forest grounds; ***paratype*** • ♀ PNM 14888 [Ornithoctoninae sp.]; Cagdianao-Basilisa, 'Mt. Arayat', Oct 2018, J Santos & GG Villancio leg.; PNM (DCA examined). *Orphnaecus kwebaburdeos* (Barrion-Dupo et al., 2015): Philippines: Polillo Is.—Quezon Prov. ***paratypes*** • 3 ♂♂ 1♀ BPB 2112012-4, BPB 2112012-12, BPB 2112012-13, BPB 2112012-2; Burdeos, [Brgy. Aluyon], Puting Bato Cave 3 & 4, 02 Nov 2012, J. Rasalan leg.; UPLB-MNH (DCA examined) • 4 ♂♂ 14♀♀ 7j UST-ARC 0059–0083; Burdeos, Brgy. Aluyon, inside Puting Bato Cave 2 & 3, 150 m horiz. depth; 13–14 May 2023, DC Acuña & JD Fornillos leg.; UST-ARC (DCA examined). *Orphnaecus* sp. 'M1': Philippines: Mindanao Is.—Agusan del Sur Prov. • 1♀ UST-ARC 0146; Prosperidad, Brgy. Poblacion, Puting Buhangin Cave-Level 3; 2019, GD Petros leg.; UST-ARC (DCA examined).

Observations and documentation were performed using an Olympus SZ61 stereo microscope with a Touptek camera attachment. Microscopic measurements were made using ToupView software version X64, while macroscopic features such as leg and body measurements were performed using digital calipers. All measurements were in millimetres to the nearest 0.01 mm and from the left sides of the spiders or mentioned otherwise. The measurement of total body length included chelicerae, but not spinnerets. The carapace length was measured from the anterior tip to the posteriormost extension (Fig. 1A).

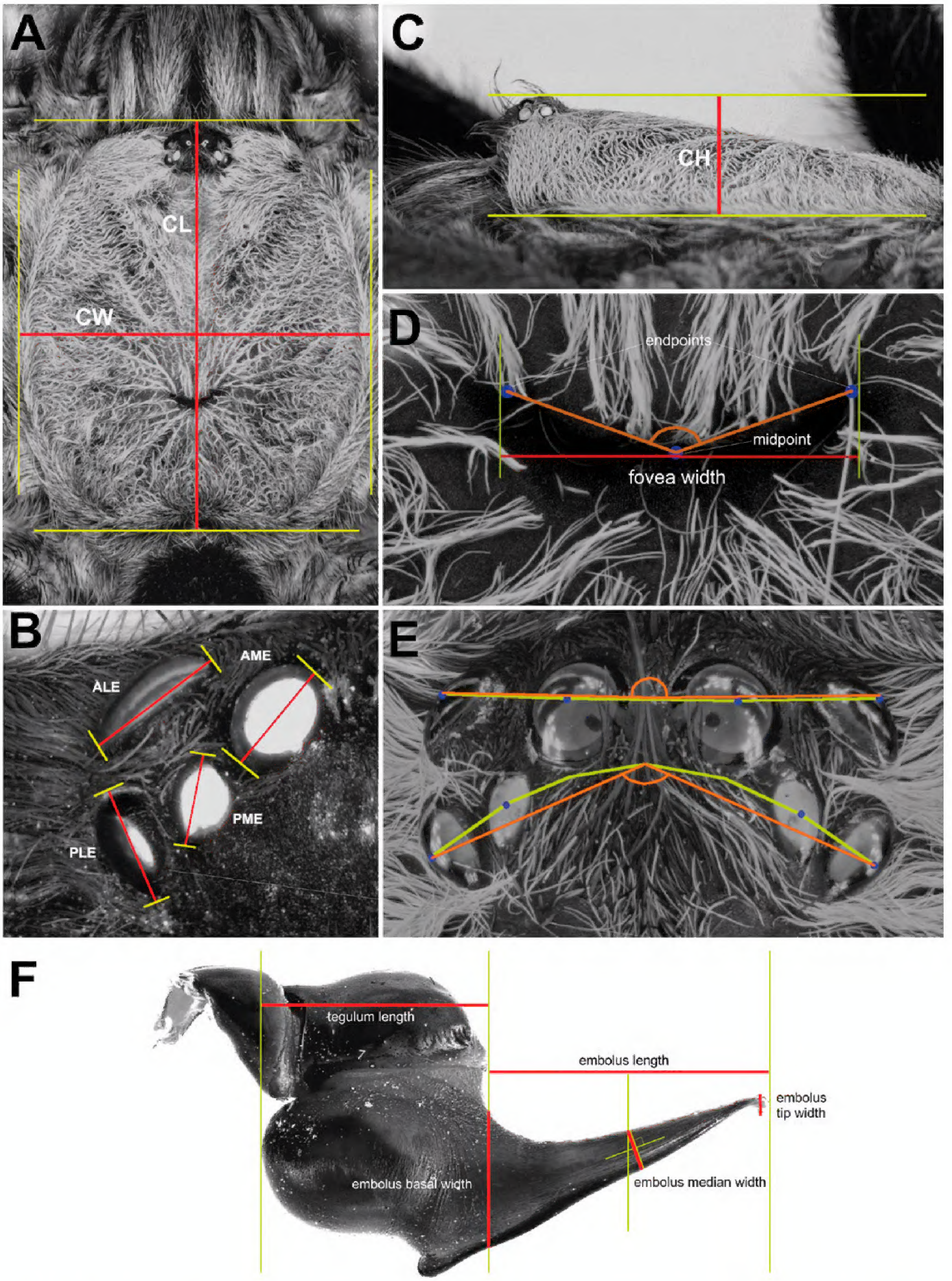

Figure 1. The morphometric methods used in this study **A** carapace length and width (red lines) **B** eye diameters on their widest point or the major axis of the eye (red lines) **C** cephalic height (red line) **D** fovea length (red line) and curvature measured by three-point angle (orange lines) **E** eye row orientation, drawn by connecting the center of eyes (blue dots) and curvature measured by three-point angle (orange lines) **F** palpal organ measurements on the prolateral view: tegulum and embolus length, embolus median width, with additional measurements of embolus basal and tip width (red lines).

The cephalic height was measured laterally from the base of the carapace to the highest point of the cephalic region (Fig. 1C). The length of the leg segments was measured on the lateral aspect up to the longest point, excluding the trochanter and coxa. Leg width was taken through the widest point, laterally. The length of the tarsus did not include claws and tufts. The widths of the tarsus and metatarsus did not include the scopulae. The length and width of the coxae and trochanter were measured ventrally. Leg formulas are the legs in descending order based on total length. The orientation of the eye rows was determined by connecting the centre or midpoint of each eye (Fig. 1E). Eye diameter (ALE, AME, PLE, and PME) was measured using the widest point or the major axis of the eye (Fig. 1B); hence, the eye measurements of *O. kwebaburdeos* and *O. adamsoni* are measured directly from type specimens and do not follow the original data in Barrion-Dupo et al. (2015) and Salamanes et al. (2022). Eye indices were computed based on the definition provided above. The Anterior Lateral Eye (ALE) index of each specimen was compared to the Anterior Median Eye (AME) index. Differences in ALE and AME for selected *Orphnaecus* species were compared and analysed. To normalise eye diameters for comparison, the eye index was used which is defined as the ratio of the eye diameter of ALE or AME to the length of the carapace. Eye indices were analysed using T-test and then plotted using ggplot using R (www.R-project.org). Fovea width was measured by drawing a straight line latitudinally (Fig. 1D). The curvature of the eye rows and fovea were given in degrees (n°) by drawing a three-point angle on the endpoints and median point of the curve (Fig. 1E).

The description of the palpal structure was based on Bertani (2009), which is based on the position of the keels. Therefore, the long retrolateral keel in the palpal embolus of male Yamiini (mentioned as Phlogiellini) in West et al. (2012) is treated here as prolateral superior keel as designated by Acuña et al. (2025). Measurements of the palpal organ were adapted from Bertani (2009), with additional measurements measured on its prolateral side (Fig. 1F). The tegulum length extended from the posterior extent of the tegulum bulb to the anterior end of the tegulum suture. The embolus length is from the anterior tip of the tegulum suture to the tip of the embolus. The basal width of embolus was measured by drawing a line on the base of embolus parallel to the tip of tegulum suture, while the median width of embolus was measured on the middle of embolus by drawing a line perpendicular to the centre line parallel to the embolus. The width of the embolus tip is the widest extent of the tip. Note that the exact division between the embolus and tegulum is hard to identify and subjective to each taxonomist, who has different interpretations of measuring the palpal organ; hence, these measurements do not represent the absolute measurements of the parts of the palpal organ but are created for uniformity in comparative morphometrics. The spermathecae were cleaned using lactic acid (von Wirth and Hildebrandt 2023).

The indices used herein were modified from Acuña et al. (2025):

CI Carapace Index = car. width/ car. length x 100, the resulting value shows the ratio of carapace width to length

CRI Cephalic Region Index = cephalic region length/ car. length x 100, the resulting value shows the length ratio of the cephalic region within the carapace

CHI Carapace Height Index = car. height/ car. length x 100, the resulting value shows the ratio of the carapace height to the length

EI Eye Index = major eye axis diameter/car. length x 100, the resulting value shows the ratio of eye diameter to carapace length

RF Leg Relation Factor (von Wirth and Striffler 1995) = total leg I length/ total leg IV length × 100, the resulting value shows the length ratio of Leg I to Leg IV

LI Leg Index = total leg I width/ total leg IV width x 100, the resulting value shows the ratio of total width to length of Leg I to Leg IV

TBI Tibia Index = tibia I length/ tibia IV length x 100, resulting value shows the length ratio of tibia I to tibia IV

TI Tarsal Index = tarsus I length/ tarsus IV length x 100, resulting value shows the length ratio of tarsus I to tarsus IV

EMI Embolic Index = Embolus length/ tegulum length x 100, the resulting value shows the length ratio of the male embolus to its tegulum

POI Palpal Organ Index = (Embolus + tegulum length)/ Palp tib. length x 100, the resulting value shows the length ratio of the male palpal organ to the palpal tibia.

SI Spermathecal Lobe Index = lobe distal width/ lobe basal width x 100, the resulting value shows the width ratio of the apex to base of the spermathecal lobe.

Description of setation of Theraphosidae utilized the terminologies of Guadanucci et al. (2020) which include the tactile setae, scales, trichobothria, epitrichobothria, chemosensory sensilla, and with additional setal terminologies from Acuña et al. (2025): Femoral setation—referred to the field of modified tactile setae on the prolateral surface of femur I (see Acuña et al. 2025, fig. 21); and Palpal scale brush—a field of acicular scales that is present on the male palpal patellae and tibiae dorsally on some Selenocosmiinae, long and dense in the male palpal patella of *Orphnaecus*. West et al. (2012) first introduced this character as a dorsal brush of dense, long setae and mentioned as 'scopulate brush' by Nunn et al. (2016). We classified them as scales owing to their weak pedicel and light-reflective scale properties (Guadanucci 2020).

The classification of the subterranean fauna followed the proposal of Sket (2008). The tolerance of tarantula spiders to hypoxia has been observed in a concurrent venom research project. In this procedure, live specimens are subjected to hypoxia before venom extraction by placing them in a 1000 mL rectangular plastic container filled with CO_2. Carbon dioxide is continuously supplied at a rate of 5 LPM (liters per minute) through a 1 cm diameter rubber tube inserted into a hole in the container's lid, connected to a 20 kg gas tank. Spiders are considered unconscious when they show no response to gentle shaking, as indicated by the absence of any observable movement. Sensitivity to ground movements was observed in situ during field sampling and in captivity in the laboratory.

Abbreviations:

A	apical keel
AE	anterior eyes
ALE	anterior lateral eye
AME	anterior median eye
BL	basal lobe
car.	carapace
cym.	cymbium
CL	carapace length
CW	carapace width
CH	carapace height
CR	cephalic region
fem.	femur
j	ungendered juvenile/s
LCNP	Libmanan Caves National Park
met.	metatarsus
OT	ocular tubercle
PE	posterior eyes
PI	inferior prolateral keel
PLE	posterior lateral eye
PME	posterior median eye
PS	superior prolateral keel
StR	subtegular ridge
tar.	tarsus
tibia	tibia
troch.	trochanter
TS	tactile setae/touch-sensitive setae
♂, ♀	one male/female
♂♂, ♀♀	two or more males/ females

Repositories:

MNHN	Muséum National d'Histoire Naturelle, Paris
PASI	Philippine Arachnological Society, Inc.-Natural History Collection, Manila
PNM	Philippine Nation Museum- Museum of Natural History, Manila
SMF	Senckenberg Museum, Frankfurt am Main
UPLB-MNH	University of the Philippines Los Baños Museum of Natural History, Laguna
UST-ARC	University of Santo Tomas - Arachnid Reference Collection, Manila

DNA isolation and amplification

DNA was isolated from tissues collected from the legs of spiders. DNA extraction was performed using the QIAGEN DNeasy Blood and Tissue Kit following the manufacturer's protocol (Qiagen, Inc., CA, USA). The degenerate primer pairs used for amplification of the cytochrome oxidase I (COI) gene were adapted from Acuña et al. (2025) and are listed in Table 1. PCR conditions included an initial denaturation at 94 °C for 3 min, followed by 5 cycles consisting of denaturation at 94 °C for 30 s, annealing at 45 °C for 30 s, extension at 72 °C for 1 min, 35 cycles of denaturation at 94 °C for 30 s, annealing at 51 °C for 1 min, extension at 72 °C for 1 min, and a final extension at 72 °C for 10 min. The amplicons were visualised on a 1.2% agarose gel. The resulting amplicons were sent to Macrogen for sequencing (Macrogen Inc., Seoul, Republic of Korea).

Phylogenetic analysis

Raw sequence data were processed using PREGAP4 and GAP4 for quality checks and trimming before alignment. Phylogenetic analysis was performed using the MEGA11 software (Tamura et al. 2021). The dataset comprised 28 sequences, including eight sequences of outgroups obtained from GenBank (Table 2), with a length of 654 base pairs. Sequences were aligned using MUSCLE with default parameters. A Maximum Likelihood (ML) tree was generated using General Time Reversible model with gamma-distributed rates and has invariant sites (GTR+G+I), chosen as the best model based on the lowest Bayesian Information Criterion (BIC) score (Nei and Kumar 2000), with 10,000 bootstrap replicates to assess node support. Genetic distances are presented as percent values (%) and were calculated using the p-distance method with uniform rates using MEGA11. Both the G and G+I rates were evaluated but yielded the same values. Although the analysis only involved the COI gene, the estimated divergence time was computed to have initial insights into their age. A TimeTree of the COI gene inferred in MEGA11 by applying the RelTime method (Tamura et al. 2012, 2018) to the generated ML tree using the same substitution model (GTR+G+I). The TimeTree was computed using a time calibration constraint at uniform distribution following the age estimates of Foley et al. (2021)

Table 1. List of primers used to amplify and sequence the DNA barcoding region COI gene.

Primers	Primer Sequence
LCO1490_PH (forward)	5'-TTTCWACTAATCATARGGATATTGG-3'
HCO2198_PH (reverse)	5'-TAAACCTCCGGATGWCCAAAAAAYCA-3'
C1-J-2123_PH (forward)	5'-GATCGAAATTTTAATACTTCKTTYTTTGA-3'
C1-J-2776_PH (reverse)	5'-GGATAATCAGAATATCGTCGAGGTATTCCAT-3'

Table 2. List of the voucher numbers and GenBank accessions of COI sequences used in the phylogenetic analysis.

Species	Voucher	GenBank Accession	Geographic range	Source
Aphonopelma seemanni	MNHN-JAC96	JN018124	Central America	GenBank: Arabi et al. 2012
Brachypelma verdezi	IBUNAM:CNNA Ar003417	KT995328	Mexico	GenBank: Barcode of Wildlife Project Mexico
Chilobrachys huahini	MNHN-JAC48	JN018125	Thailand	GenBank: Arabi et al. 2012
Chilobrachys sp.	USNM ENT 01117339	MF804598	Myanmar	GenBank: B Blaimer and DG Mulcahy (submitter)
Chilobrachys sp.	NIBGE SPD-00687	JF884459	Pakistan	GenBank: International Barcode of Life
Grammostola rosea	NCA 2017/394	MK234708	South America	GenBank: Shivambu et al. 2020
Grammostola sp.	JEA-2015	KT022078	Chile	GenBank: Mieres
Orphnaecus kwebaburdeos	UST-ARC 0061 (QB1-03)	PQ578695	Polillo Is., Philippines	this study
Orphnaecus kwebaburdeos	UST-ARC 0064 (QB1-06)	PP778328	Polillo Is., Philippines	this study
Orphnaecus kwebaburdeos	UST-ARC 0065 (QB1-07)	PQ578696	Polillo Is., Philippines	this study
Orphnaecus kwebaburdeos	UST-ARC 0068 (QB1-10)	PQ578697	Polillo Is., Philippines	this study
Orphnaecus kwebaburdeos	UST-ARC 0081 (QB2-07)	PP778329	Polillo Is., Philippines	this study
Orphnaecus libmanan sp. nov.	UST-ARC 0130 (CSL02-01)	PP778307	Bicol Peninsula, Philippines	this study
Orphnaecus libmanan sp. nov.	PNM 18868 (UST-ARC 0134, field#CSL04-01)	PP778308	Bicol Peninsula, Philippines	this study
Orphnaecus libmanan sp. nov.	UST-ARC 0135 (CSL04-02)	PP778309	Bicol Peninsula, Philippines	this study
Orphnaecus libmanan sp. nov.	UST-ARC 0136 (CSL04-03)	PP778310	Bicol Peninsula, Philippines	this study
Orphnaecus libmanan sp. nov.	UST-ARC 0137 (CSL04-04)	PP778311	Bicol Peninsula, Philippines	this study
Orphnaecus libmanan sp. nov.	UST-ARC 0138 (CSL04-05)	PP778312	Bicol Peninsula, Philippines	this study
Orphnaecus pellitus	UST-ARC 0031 (CSL01-01)	PP778304	Bicol Peninsula, Philippines	this study
Orphnaecus pellitus	UST-ARC 0032 (CSL01-02)	PP778305	Bicol Peninsula, Philippines	this study
Orphnaecus pellitus	UST-ARC 0038 (CSL01-08)	PP778306	Bicol Peninsula, Philippines	this study
Orphnaecus pellitus	UST-ARC 0052 (CSL05-01)	PP778313	Bicol Peninsula, Philippines	this study
Orphnaecus pellitus	UST-ARC 0057 (CSL05-06)	PP778314	Bicol Peninsula, Philippines	this study
Orphnaecus pellitus	UST-ARC 0058 (CSL05-07)	PP778315	Bicol Peninsula, Philippines	this study
Selenobrachys philippinus	UST-ARC 0112 (NOM1A-01)	PP778324	Negros Is., Philippines	this study
Selenobrachys philippinus	UST-ARC 0115 (NOM1A-04)	PP778325	Negros Is., Philippines	this study
Orphnaecus tangcongvaca sp. nov.	PNM 18869 (UST-ARC 0142, field#CSL06-02)	PP778316	Bicol Peninsula, Philippines	this study
Orphnaecus sp.	UST-ARC 0146 (PBAT1-01)	PP778326	Mindanao Is., Philippines	this study

between the split of Selenocosmiinae and Theraphosinae (106.5 Ma–111 Ma). Bars around selected nodes represent 95% confidence intervals (CI). The phylogenetic network of the same COI sequences was generated using SPLITSTREE (Huson and Bryant 2024) to gain a have deeper understanding of species divergence and to reveal complex evolutionary relationships which are not captured by the traditional phylogenetic trees by effectively representing complex evolutionary processes like hybridisation, horizontal gene transfer, and recombination, providing a more accurate depiction of genetic diversity and reticulate relationships (Posada and Crandall 2001; Bryant and Moulton 2004; Huson and Bryant 2006).

Results

Based on morphological and phylogenetic analyses performed on the tarantulas collected from LCNP, three species of tarantula spiders inhabit LCNP. One of the species, the previously described *Orphnaecus pellitus*, was exclusively collected inside the cave systems, whereas the other two species, *Orphnaecus libmanan* sp. nov. and *Orphnaecus tangcongvaca* sp. nov., inhabit the forest grounds of the LCNP and adjacent areas. The dorsal habitus of the three species is shown in Fig. 2.

Troglomorphism and subterranean adaptations of *O. pellitus*

New specimens of *O. pellitus* were collected from the type locality in the three interconnected caves of the Culapnitan Cave system in LCNP—Alinsanay Cave, Kalangkawan Cave, and Laya Cave in the dark zones (no penetration of light) at 30–300 m horizontal depth. Troglomorphic traits and other subterranean adaptations have also been observed.

***Orphnaecus pellitus* Simon, 1892**
Figs 2A, B, 3, 5

Orphnaecus pellitus Simon, 1892 (Simon 1892: 36; Simon 1903: 956, figs 1106–1107; West et al. 2012: 25, figs 35a–c; Acuña et al. 2025: figs 15a, 20g).

Type material examined. ***Syntypes*** • 1♂ 2♀♀ MNHN AR4678; Philippines: Luzon Island, Bicol Peninsula, Camarines Sur Province, Libmanan, 'Calapnitan Caves' [Culapnitan Caves] (now Libmanan Caves National Park). (VVW examined syntypes ♂♀; A.-E. Leguin sent images of another syntype ♀) (VVW examined syntypes ♂♀; A.-E. Leguin sent images of another syntype ♀).

Other material examined. • 2♂♂ 3♀♀ 12j, UST-ARC 0031–0047; Philippines: Luzon Island, Bicol Peninsula, Camarines Sur Prov., Libmanan, Brgy. Sigamot, Libmanan Caves National Park (Culapnitan Caves), inside Kalangkawan Cave; 50–300 m horiz. depth, 20 Apr 2023, LA Guevarra, DC Acuña, CN Noriega, JD Fornillos leg. • 4j UST-ARC 0048–0051; [same general locality data as for above], inside Alinsanay Cave; 50 m horiz. depth, [same collection data as for above] • 2♂♂ 4♀♀ 1j, UST-ARC 0052–0058; [same general locality data as for the former], inside Laya Cave; 30–50 m horiz. depth, 20 July 2023, LA Guevarra, DC Acuña, JD Fornillos leg. (DCA examined).

Gene sequence. GenBank accessions: PP778304–PP778306 and PP778313–PP778315 (non-types).

Troglomorphism. The troglomorphic characters of *O. pellitus* are presented in Figs 3, 4. A noticeable troglomorphic characteristic of *O. pellitus* is its weakly pronounced ocular tubercles. Adult specimens of *O. pellitus* have distinctly tiny

Figure 2. Dorsal habitus of theraphosid species of LCNP **A** *Orphnaecus pellitus*, female **B** mature male **C** *Orphnaecus tangcongvaca* sp. nov., holotype female **D** *Orphnaecus libmanan* sp. nov., paratype female **E** holotype male. Note: Size on actual scale.

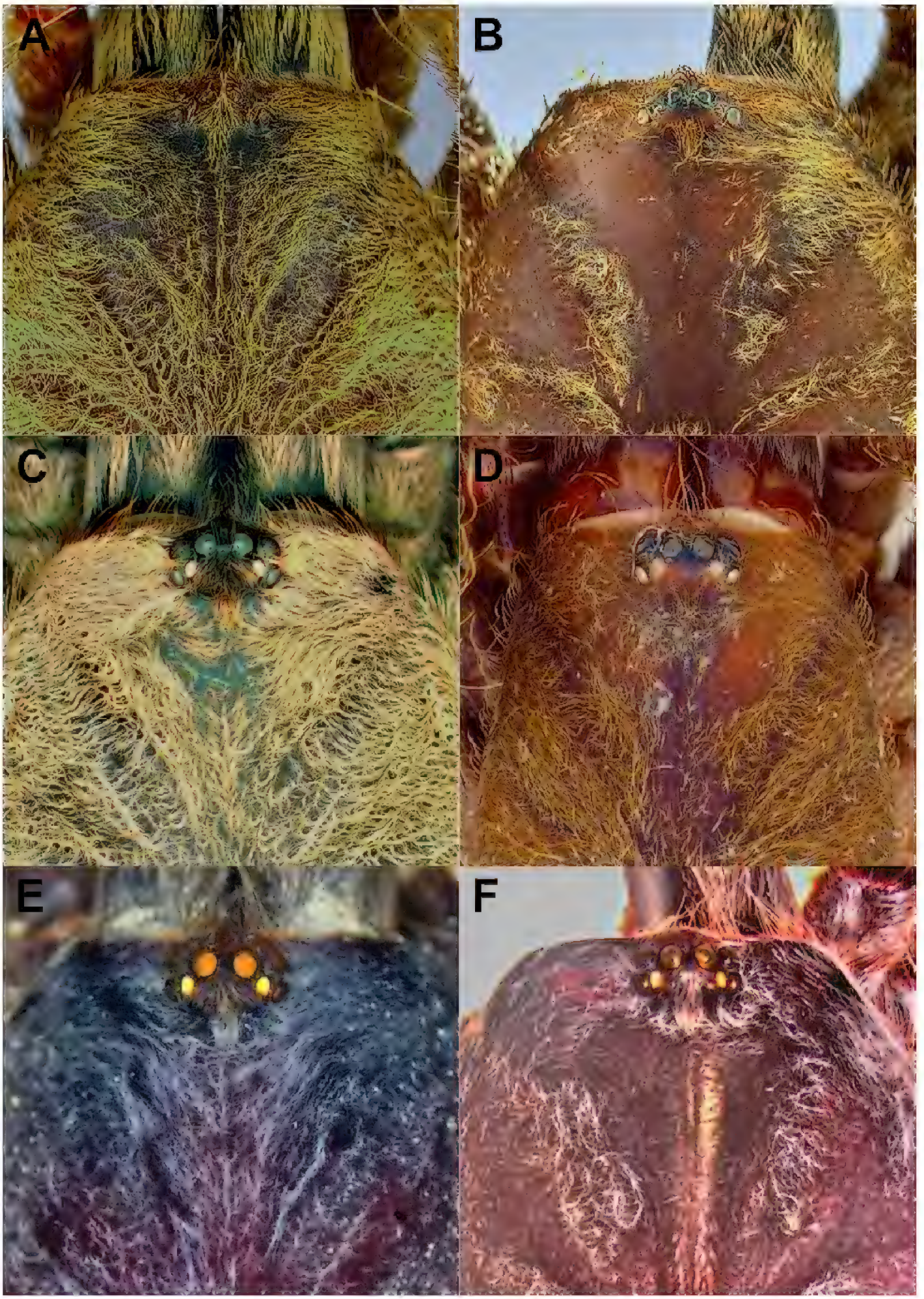

Figure 3. Anterior carapace of all known *Orphnaecus* species showing the comparison of ocular tubercles **A, B** *O. pellitus*, showing variation in eyes **A** ♂ UST-ARC 0055 **B** ♂ UST-ARC 0052 **C** *O. libmanan* sp. nov., holotype ♂ UST-ARC 0133 **D** *O. tangcongvaca* sp. nov., holotype ♀ UST-ARC 0142 **E** *O. kwebaburdeos*, paratype ♂ BPB 2112012-13 **F** *O. adamsoni*, holotype ♂ PNM 14889.

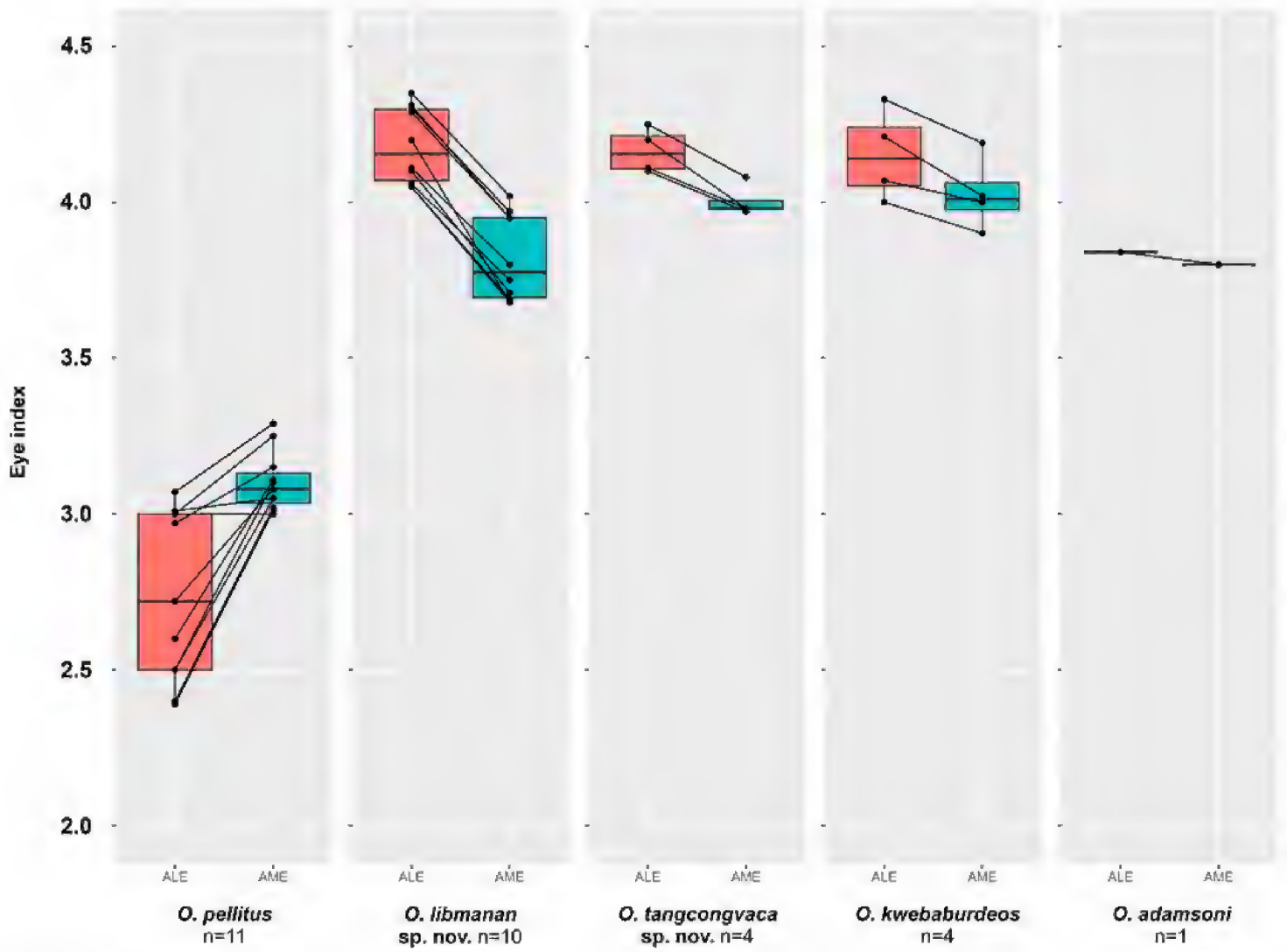

Figure 4. Eye indices (AME and ALE) of selected *Orphnaecus* species. Connecting lines denote the same individual. The ALE and AME diameter of *O. pellitus* are relatively smaller than its epigean and troglophile congeners and the ALE ≤ AME based on EI values. Note: Eye index is the ratio of the eye diameter of ALE or AME to the length of the carapace.

eyes making interocular distances greater than epigean and troglophilic congeners (Fig. 3). The AME and ALE range are 3.01–3.29 and 2.39–3.07, respectively. Lower ALE, as compared to AME, was only observed in *O. pellitus* but not in its congeners, suggesting that the eye morphology of *O. pellitus* is different from that of other *Orphnaecus* species (Fig. 4).

The colour of the body integuments of *O. pellitus* is lighter (brown) than that of other *Orphnaecus* species we recently collected and examined. The microstructures of the scales are greyish to dark brown and lack the typical purplish to dark blue sheen of the typical epigean *Orphnaecus* species. Both mature males and females had shorter leg I than leg IV with a leg formula of 4123 and RF ~99 (n = 15). The legs were stout and elongated. The tactile setae all over the body and appendages were also noticeably shorter.

Other subterranean adaptations. After subjecting live specimens of *O. pellitus* to hypoxia, we observed that they took 5–12 min before they completely lost consciousness and became motionless. On the other hand, epigean and troglophile species subjected to the same procedure became unresponsive less than 2 min after exposure to high CO_2 concentrations. Individuals were also observed to recover faster than non-troglobitic congeners, with no fatalities recorded.

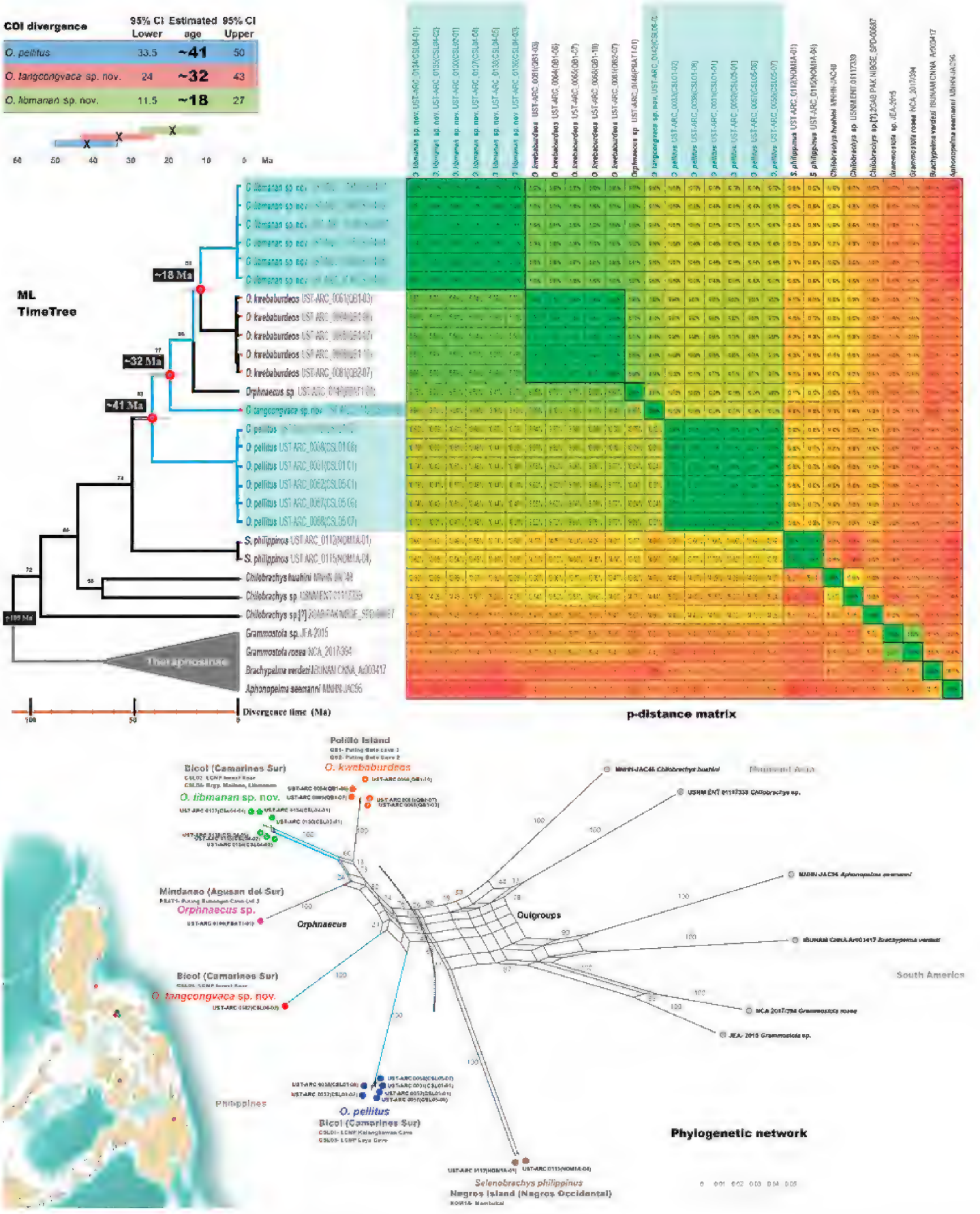

Figure 5. The heterospecificity of the three species in LCNP is well supported in the phylogenetic analysis, in which divergences started from ~41Ma (Middle Eocene) to ~18Ma (Early Miocene). The estimated divergence time of the COI gene of the different species of LCNP is represented by 95% confidence intervals (CI), and the time is expressed in million years ago (Ma) (upper corner left). The Timetree was calculated using the Maximum Likelihood (ML) method and has bootstrap values, divergence time estimates, and error bars (pink) representing 95% CI (upper left). Species divergences in LCNP are highlighted in pale blue in the ML tree and network, and divergences (nodes) of species in LCNP are marked with red dots in the ML tree. The p-distance heatmap matrix (upper right) with genetic distances is expressed in percentage. The generated phylogenetic network of the same COI gene sequences of different *Orphanecus* species and outgroups (lower right). The distribution map shows the locations of the analyzed sequences (lower left). Philippine relief map: © 2024 Mapsland.

Field observations indicate heightened sensitivity to ground movements in the surrounding environment. When the tarantulas were collected in the caves of the LCNP, they quickly retreated into their burrows when approached from more than a meter away, a behavior not observed in epigean species during our field sampling. In the laboratory, these tarantulas demonstrated rapid prey detection and capture behaviour when fed live insects (*Blaptica dubia*, *Blatta lateralis*, and Gryllidae). The live insects were introduced into their plastic enclosure and as soon as the insects touched the ground of the substrate, the spiders promptly captured their prey without pausing to observe their surroundings consistently. Notably, juveniles could prey on insects three times their body size. These behaviours could be attributed to the increased sensitivity of their ground movement-sensitive clavate trichobothria and their opportunistic instinct towards food in an environment with limited resources.

Remarks. This study focused only on the troglomorphic characteristics of *O. pellitus*. Redescription of this species is being conducted in an ongoing study on the revision of the genus *Orphnaecus*.

Phylogenetic analysis

To determine the phylogenetic relationship and verify the heterospecificity and taxonomic placement of the species in the LCNP, we analysed 28 COI gene sequences. These included 21 sequences from our Philippine tarantula collection, three from other Asian taxa, and four from Neotropic taxa outgroups. Fig. 5 presents the results of the phylogenetic analysis.

The Maximum Likelihood tree topology showed that all species in the LCNP emerged within the *Orphnaecus* clade and revealed three divergences in the LCNP. Based on the TimeTree, the possible first split based on COI divergence time estimates is by the troglobitic *O. pellitus*, probably at 33.5–50 Ma, then followed by the dwarf species, *O. tangcongvaca* sp. nov. probably at 24–43 Ma, and recently, probably at 11.5–27 Ma, by the typical epigean *O. libmanan* sp. nov. The p-distance values support the heterospecificity of the three species. The intraspecific genetic distances ranged from 0% to 0.46% within each analysed *Orphnaecus* species. The interspecific genetic distances between *Orphnaecus* species were > 5%. The genetic distance between *O. pellitus* and *O. tangcongvaca* sp. nov. ranges from 10.08%–10.31%, and that between *O. pellitus* and *O. libmanan* sp. nov. ranges from 10.21%–10.79%. The genetic distance between *O. tangcongvaca* sp. nov. and *O. libmanan* sp. nov. ranged from 9.09% to 9.72%. Although the bootstrap value between *O. libmanan* sp. nov. and *O. kwebaburdeos* clades is only 51, the genetic distance between the samples from these species ranges from 5.41%–5.86%, which suggests their close relationship and most recent split among known *Orphnaecus* species. On the other hand, divergences of *O. pellitus* and the clade including *O. tangcongvaca* sp. nov. have good support with bs = 83 and 77, respectively. The ML tree topology and genetic distances support conspecificity between the populations of *O. pellitus* in Kalangkawan Cave (voucher UST-ARC 0031, 0032, and 0038 in the ML Tree) and Laya Cave (vouchers UST-ARC 0052, 0057, and 0058)

with a maximum p-distance of 0.33%. The resulting phylogenetic network also supports the heterospecificity among the three *Orphnaecus* species in the LCNP. The dwarf *O. tangcongvaca* sp. nov. was consistently placed within the *Orphnaecus* clade. The close split between *O. libmanan* sp. nov. and *O. kwebaburdeos* was also consistently supported in the phylogenetic network. Overall, the ML tree topology, genetic distances, and phylogenetic network based on the COI gene support heterospecificity among the three divergences in the LCNP, with divergences occurring at different geologic times, possibly from the Middle Eocene (~41Ma) until the Early Miocene epoch (~18Ma).

Description of the two new species of LCNP

Two new species of *Orphnaecus*, *O. libmanan* sp. nov., and *O. tangcongvaca* sp. nov., were collected from the forest of LCNP. *O. libmanan* sp. nov. is a regular-sized tarantula collected from two sampling areas, within the forest grounds of LCNP (the nearest sample collected from the mouth of the caves is approximately 10 m away) and the other is from Sitio Guimbal, Barangay Malinao (4.5 kilometers from LCNP), while *O. tangcongvaca* sp. nov., is a dwarf tarantula collected from LCNP grounds. The two new species of *Orphnaecus* are described below.

Taxonomy

Family Theraphosidae Thorell, 1869

Subfamily Selenocosmiinae Simon, 1889

Included tribes. Chilobrachini West et al., 2012, Selenocosmiini Simon, 1889, Yamiini Kishida, 1920.

Tribe Yamiini Kishida, 1920

Phlogiellini West et al., 2012 (synonymized by Nunn et al. 2016).

Included genera. *Orphnaecus* Simon, 1892, *Phlogiellus* Pocock, 1897, *Selenobrachys* Schmidt, 1999.

Genus *Orphnaecus* Simon, 1892

Orphnaecus Simon, 1892 (Simon 1892, 36; Simon 1903: 956; West et al. 2012: 25, Acuña et al. 2025).

Type species. *Orphnaecus pellitus* Simon, 1892, by monotypy.

Included species: *O. adamsoni* Salamanes et al., 2022, *O. kwebaburdeos* (Barrion-Dupo et al., 2015), *O. pellitus* Simon, 1892, *O. libmanan* sp. nov., *O. tangcongvaca* sp. nov.

Diagnosis. See Acuña et al. (2025).

Orphnaecus libmanan Acuña & Guevarra, sp. nov.

https://zoobank.org/4850F4A4-B914-4D1F-BD5F-FC3322680E34

Figs 5–8

Orphnaecus sp. "L3" Acuña et al., 2025.

Type material. ***Holotype*** • ♂ PNM 18867 UST-ARC 0133, field#CSL02-04, ***Paratype*** • ♀ UST-ARC 0132 (field#CSL02-03); Philippines: Luzon Island, Bicol Peninsula, Camarines Sur Prov., Libmanan, Brgy. Sigamot, Libmanan Caves National Park; burrows under and inside rotten logs on forest slope near Kalangkawan Cave, 20 Jul 2023, LA Guevarra, DC Acuña, JD Fornillos leg. ***Paratypes*** • ♂♀, UST-ARC 0130–0131 (field# CSL02-01–02); [same locality and natural history data as for holotype]; 20 Apr 2023, LA Guevarra, DC Acuña, CN Noriega, JD Fornillos leg. ***Paratype*** • ♀ PNM 18868 UST-ARC 0134. field#CSL04-01; [same general locality as for holotype], Brgy. Malinao, Sitio Guimbal, burrow under limestone rock; 20 Apr 2023, LA Guevarra, DC Acuña, CN Noriega, JD Fornillos leg. ***Paratypes*** • 3♂♂ 3♀♀, UST-ARC 0135–0140 (field# CSL04-02–07); [same locality data as for the latter], 20 Jul 2023, burrows under piles of coconut husks; LA Guevarra, DC Acuña, JD Fornillos leg. (DCA examined).

Type gene sequence. GenBank accessions: PP778307–PP778312 (paratypes).

Diagnosis. *O. libmanan* sp. nov. belongs to the genus *Orphnaecus* for having reniform lyrate morphology with a row of club-shaped stridulatory setae (Figs 5G, H, I, 7H), palpal organ with embolus having basal lobe and PS keel from tip to base (Fig. 6B–F), presence of palpal scale brush on patellae in males (Fig. 6A). Females of *O. libmanan* sp. nov. differ from those of *O. kwebaburdeos*, *O. pellitus*, and *O. tangcongvaca* sp. nov. in having a relatively narrower apex than the base of the spermathecal lobe (SI ~44, n = 6; SI > 55 in the mentioned congeners) (Fig. 8C), in having a greater number of mesoventral denticles with > 100 (n = 6) (<60 in mentioned congeners), and in having relatively longer tarsus I than IV (TI ~118, n = 6; T < 112 in mentioned congeners). The females further differed from *O. kwebaburdeos* and *O. tangcongvaca* sp. nov. in having relatively shorter tibia I than IV (TBI ~90, n = 6; TBI > 104 in the mentioned congeners). The females also differed from *O. kwebaburdeos* in having a relatively shorter leg I than IV (RF ~95, n = 6; slightly longer leg I than IV in *O. kwebaburdeos* females, RF ~101). Mature males of *O. libmanan* sp. nov. differ from mature males of *O. adamsoni*, *O. kwebaburdeos*, and *O. pellitus* in having a relatively shorter embolus than the tegulum (EMI ~112, n = 5; EMI > 120 in the mentioned congeners) and longer leg I than IV (RF ~102, n = 5; shorter leg I than IV in the mentioned congeners, RF ~99). The mature males further differed from *O. adamsoni* and *O. kwebaburdeos* in having relatively longer tarsus I than IV (TI ~108, n = 5; shorter

tarsus I than tarsus IV in the mentioned congeners, TI < 93). *O. libmanan* sp. nov. also differs from *O. pellitus* and *O. tangcongvaca* sp. nov. in that it does not exhibit troglomorphism and dwarfism, respectively.

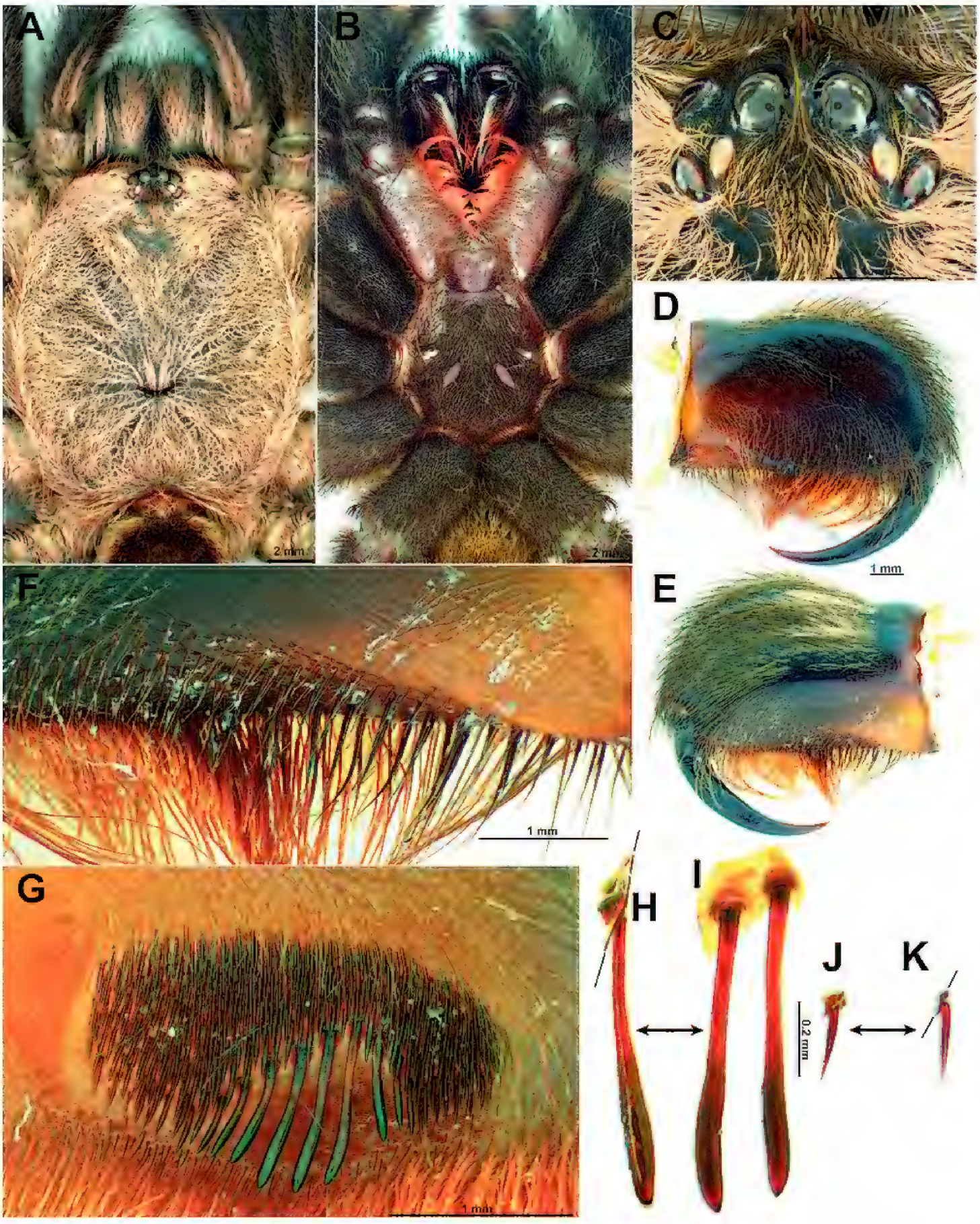

Figure 6. *Orphnaecus libmanan* sp. nov., holotype ♂ **A** prosoma, dorsal view **B** ventral view **C** ocular tubercle, dorsal view **D** left chelicera, prolateral view **E** retrolateral view **F** cheliceral strikers, retrolateral view **G** lyra (stridulatory organ), on prolateral maxillary surface **H** largest stridulatory setae of lyra, prolateral view **I** dorsal view **J** smallest stridulatory seta on lyra, dorsal view **K** prolateral view.

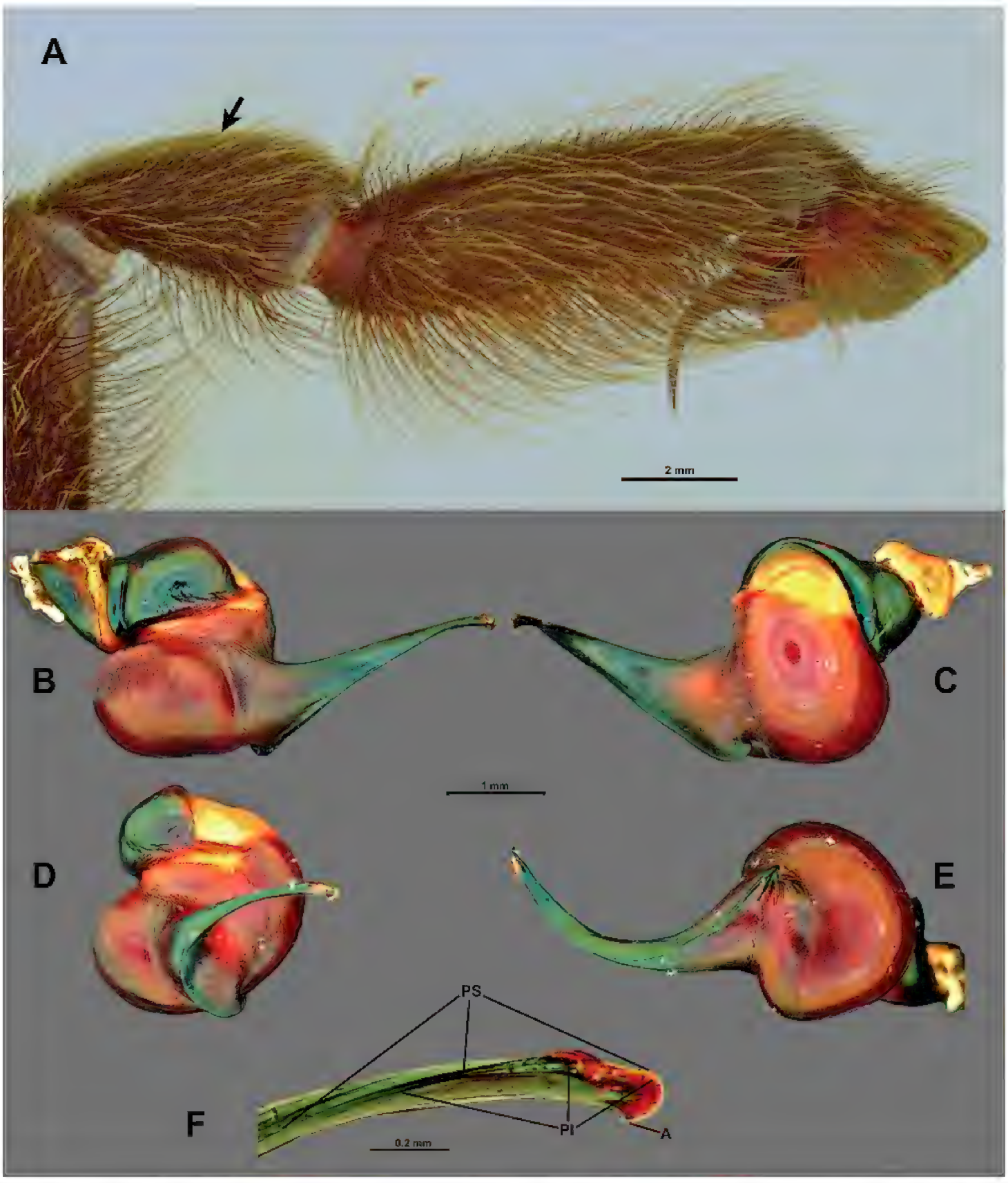

Figure 7. *Orphnaecus libmanan* sp. nov., holotype ♂ pedipalp and palpal organ **A** left pedipalp, prolateral view, showing the dense palpal scale brush (arrow) **B** left palpal organ, prolateral view **C** retrolateral view **D** apical view **E** ventral view **F** tip of embolus, prolateral view. Abbreviations: PS = prolateral superior keel, PI = prolateral inferior keel, A = apical keel.

Remarks. The female of *O. adamsoni* Salamanes et al., 2022 was not distinguished from *O. libmanan* sp. nov. and all known *Orphnaecus* species because the paratype female is misidentified and misplaced in *Orphnaecus.* The allotype/paratype ♀ (PNM 14888) used in the original description of the female (Salamanes et al. 2022) is also misplaced in *Orphnaecus.* Rather, it belongs to Ornithoctoninae because of the presence of a plumose

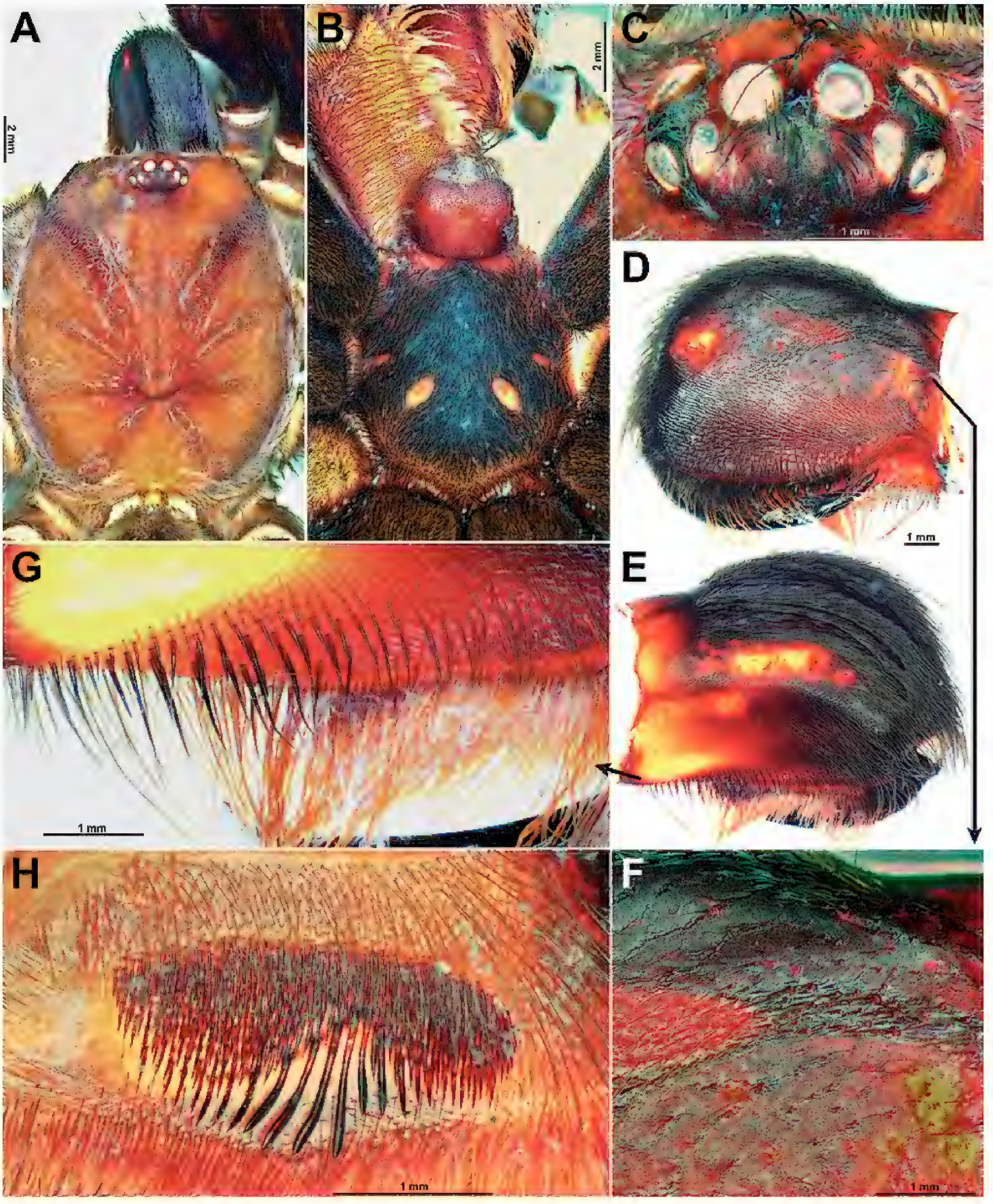

Figure 8. *Orphnaecus libmanan* sp. nov., paratype ♀ prosoma **A** prosoma, dorsal view **B** ventral view **C** ocular tubercle, dorsal view **D** right chelicera, prolateral view, **E** retrolateral view **F** intercheliceral setae on right prolateral chelicera **G** cheliceral strikers on right chelicera, retrolateral view **H** maxillary lyra (stridulatory organ), prolateral view.

setal field on retrolateral chelicerae, rows of thorn stridulatory setae on the prolateral maxilla, conspicuous white bands on leg segments, and stripe patterns on the dorsal abdomen, which are characteristics absent in Selenocosmiinae but synapomorphic to Ornithoctoninae. This specimen probably represents an undescribed *Melognathus* species,

but a new taxon cannot be assigned to this specimen owing to its poor condition. Other paratype females could potentially be available to the species authors' institution, but no response has been received to date from our multiple enquiries sent to the first author.

Description holotype male. PNM 18867 UST-ARC 0122, field#CSL02-04, body length 36.02. (Figs 5, 6).

Prosoma. Carapace (Fig. 6A): CL 14.45, CW 12.52, CH 4.72, CR 10.05 long, lateral profile low and flat, and integument matte black. Fovea (Fig. 6A): width 1.55, curvature at 143°, procurved. Ocular Tubercle: 1.99 long, 2.6 wide. Eyes (Fig. 6C): AME round, ALE, PME, and PLE ovoid, clypeus almost absent. AE row almost straight at 176°, PE row recurved at 139°. Eye diameters, AME 0.64, ALE 0.67, PME 0.52, PLE 0.56. Interocular distances, AME–AME 0.21, ALE–ALE 1.72, PME–PME 1.31, PLE–PLE 1.87, AME–ALE 0.2, AME–PME 0.13, AME–PLE 0.48, ALE–PLE 0.23, ALE–PME 0.31, PME–PLE 0.07. Chelicerae (Fig. 6D–F): length 8.32, width 5.20, fang curve length 6.28, teeth 10, mesoventral denticles ~40. Cheliceral strikers (Fig. 6F): primary rows, ~13, 0.68–1.07 long, dark long spiniform with filiform ends. Secondary rows, ~30, 0.29–0.73 long, dark short spiniform with filiform ends. Tertiary rows, ~83, 0.20–0.75 long, pallid tiny needleform. Pseudostrikers, pallid and present ventrally. Maxillae (Fig. 6G): prolateral maxilla 5.23 long, 3.74 wide laterally, 3.46 wide ventrally. Maxilla prolaterally planoconvex, anterior lobe well pronounced. Maxillary cuspules ~272. Lyra (Fig. 6G, F): lyrate patch 2.33 long, 1.40 high, with a total of ~366 stridulatory setae, in 10 or 11 rows, surrounded by fine setae, denser above and distally. Short pointed stridulatory setae (Fig. 6J, K) ~361, 0.12–0.41 long, forming reniform patch, proximally broad. The largest stridulatory setae nine (Fig. 6H, I), 0.60–0.92 long, situated at the lowest row medially, with the median three are larger and with weakly pointed and well-defined paddle blades, and with stout shaft laterally. Labium: 2.10 long, 2.77 wide, integument reddish brown, anterior 1/3 with cuspules ~514. Sternum (Fig. 6B): 7.47 long, 6.83 wide. Sternal corners mildly acuminate, posterior corner acuminate. Labiosternal sigilla 1.20 long, 0.50 wide, 0.40 apart. Sternal sigilla 3 pairs, anterior sigilla 0.33 long, 0.23 wide, 4.47 apart, and 0.40 away from sternal margin adjacent to coxa I, median sigilla 0.93 long, 0.30 wide, 3.57 apart, and 0.63 away from sternal margin adjacent to coxa II, posterior sigilla 1.40 long, 0.53 wide, 1.60 apart, and 1.27 away from sternal margin adjacent to coxa II.

Opisthosoma. Abdomen: 13.02 long, 3.97 wide, ovular elongated, integument pale brown. Spinnerets: PMS 2.00 long, 0.59 wide, PLS basal segment 3.15 long, 1.36 wide, median segment 2.05 long, 1.12 wide, apical segment 3.17 long, 0.83 wide.

Genitalia. Palpal organ (Fig. 7): length almost 1/2 of palp tibia length (POI 46.32). Tegulum 1.96 long, globular, widest medially, prolaterally pronounced, subtegular projection (StR) weakly pronounced. Embolus length 2.19, basal width 0.69, median width 0.21, tip 0.13 wide. Embolus length ~1.12 times longer than tegulum length (EMI 111.74), base broad, tapering distally, and curved retrolaterally. Embolus has a long prolateral superior keel (PS) from base to tip, broad basally and at the tip (Fig. 6B–F); has short and stout prolateral inferior keel (PI), emerged from the tip to rear at around apical 1/4, located below PS and embolic opening (Op) (Fig. 6F); apical

keel (A) very short, emerged at the tip (Fig. 6F); embolic opening (Op) located between PS and PI near the tip (Fig. 6F). Basal lobe is pronounced and broad (Fig. 7B–F).

Legs. Leg formula 1423. Leg lengths (fem. pat., tib., met., tar./cym.): palp 26.12 (9.12, 4.84, 8.96, n/a, 3.20), leg I 49.44 (13.19, 7.11, 12.84, 9.73, 6.57), leg II 42.69 (11.94, 5.43, 10.87, 8.96, 5.49), leg III 36.72 (9.43, 4.36, 8.12, 9.08, 5.73), leg IV 48.42 (12.36, 5.43, 11.70, 12.84, 6.09). Leg widths (fem. pat., tib., met., tar./cym.): palp (2.68, 2.48, 2.76, n/a, 3.24), leg I (3.52, 2.99, 2.51, 1.73, 1.19), leg II (3.22, 2.69, 2.21, 1.31, 1.13), leg III (2.93, 2.39, 1.97, 1.49, 1.19), leg IV (2.87, 2.69, 2.09, 1.31, 1.08). Tarsi III and IV with transverse weakening (cracked or bent), tarsi I and II with no visible weakening. Spines: Metatarsal spines (dorsal-ventral), met. I and II absent, met. III and IV 2, 3. Claws: all tarsal claws with 2 or 3 teeth, tarsus IV with unpaired inferior third claw.

Setation. Tactile setae (TS)—carapace entirely with rows of very short brownish-white TS (Fig. 6A). Carapace margin, dorsal and upper 1/2 retrolateral surface of chelicerae, ventral prosoma, opisthosoma, and legs covered with dark and grayish brown, long and short TS, denser on abdomen and all ventral tibiae. Mesoprolateral surface of chelicerae with intercheliceral setae in arcuate strip of rows of setae basally spiniform and anteriorly filiform (Fig. 6D). Above maxillary suture with rows of short spiniform setae, retrolateral surface smooth with vertical striation on distal 1/4 and with rows of fine pallid setae ventrolaterally, and proximal end of prolateral surface with sparse very short spiniform setae. Femoral setation, dark and needleform, intermixed with regular TS. Scales—carapace, basodorsal surface of chelicerae, coxae, trochantera, and femora dorsally with pale beige to pale brown cottony and wavy fine scales, proximally grayish-brown on dorsal femora (Fig. 6A,B,E). Chelicerae, dorsal and upper retrolateral surface, dorsal maxilla, sternum, abdomen, dorsal PLS legs, covered with grayish-brown to grayish white lanceolate flat scales, which reflect purplish blue sheen, except on ventral abdomen and prolateral femora. Palpal scale brush, grayish white, present on patella and tibia, dorsally, very long and dense on patellae (Fig. 6A). Trichobothria—clavate trichobothria present on all leg tarsi and cymbium, intermixed with epitrichobothria. Epitrichobothria clusters were present on all metatarsi, tarsi, and tibiae. Filiform trichobothria were sparsely present on all dorsal legs. Chemosensory sensilla—present sparsely all over the body and legs except on the carapace and chelicerae, dense on the scopulae field. Scopulae: cymbium entire; tar. I–III entire, undivided but intermixed with one or two rows of short stiff setae; tar. IV, entire, divided by four or five rows of long stiff setae; met. I–III, almost entire, undivided but sparsely intermixed with long TS; met. IV, covering 3/4, divided by two or three rows of long setae.

Color. Bicolored: the legs and opisthosoma are dark, while the carapace, coxae, and trochantera are pale brown to pale beige dorsally. The microstructures of the scales on the legs and abdomen reflect a purplish-blue sheen, and the scales on the carapace reflect a pinkish sheen (Fig. 6A). The integument of the carapace is matte black. As the exoskeleton aged, the specimen became entirely dark brown before ecdysis.

Indices. CI 86.64, CHI 32.66, CRI 69.55, EI (AME) 4.43, EI (ALE) 4.64, RF 102.11, LI 118.92, TBI 109.74, TI 107.88, EMI 111.74, POI 46.32.

Description paratype female. PNM 18868 UST-ARC 0134, field# CSL04-01, body length 40.36. (Figs 8, 9)

Prosoma. Carapace (Fig. 8A): CL 16.30, CW 13.05, CH 4.84, CR 11.25 long, lateral profile low and flat, and integument reddish brown. Fovea (Fig. 8A): 2.12 wide, curvature 134°, procurved. Ocular tubercle (Fig. 8C): 2.04 long, 2.8 wide. Eyes (Fig. 8C): AME round, while ALE, PME, and PLE ovoid, clypeus almost absent. AE row slightly procurved at 165°, and PE row recurved at 146°. Eye diameters, AME 0.60, ALE 0.66, PME 0.55, PLE 0.52. Interocular distances, AME-AME 0.34, ALE-ALE 1.77, PME-PME 1.42, PLE-PLE 2.11, AME-ALE 0.24, AME-PME 0.14, AME-PLE 0.61, ALE-PLE 0.29, ALE-PME 0.29, PME-PLE 0.07. Chelicerae (Fig. 8D–G): length 9.16, width 6.8, fang curve length 7.96, teeth 14 (ten large, four small), mesoventral denticles dense ~122. Cheliceral strikers (Fig. 8G): primary rows, ~9, 0.82–1.20 long, dark long spiniform with filiform ends. Secondary rows, ~46, 0.29–0.72 long, composed of dark long and short spiniform strikers, rows anteriorly with filiform ends. Tertiary rows, ~65, 0.22–0.62 long, pallid tiny needleform setae. Pseudostrikers, pallid and present ventrally. Maxillae (Fig. 8H): 6.48 long, 4.40 wide laterally, 3.40 wide ventrally. Maxilla prolaterally planoconvex, anterior lobe well pronounced, maxillary cuspules ~337. Lyra: lyrate patch, 2.56 long, 1.36 high, total stridulatory setae ~390, surrounded by very fine setae, denser above and distally. Short stridulatory setae ~375, forming reniform patch. Largest stridulatory setae 10, situated at the lowest row medially, with the median three are larger and club-shaped with weakly pointed and well-defined paddle blades, and with stout shaft laterally. Labium (Fig. 8B): 2.48 long, 3.28 wide, integument reddish brown, and anterior 1/3 with cuspules ~728. Sternum (Fig. 8B): 7.88 long, 6.68 wide, sternal corners mildly acuminate, and posterior corner acuminate. Labiosternal sigilla 1.35 long, 0.50 wide, 0.49 apart. Sternal sigilla three pairs, anterior sigilla 0.44 long, 0.24 wide, 4.40 apart, and 0.27 away from sternal margin adjacent to coxa I, median sigilla 0.79 long, 0. 32 wide, 4.13 apart, and 0.63 away from sternal margin adjacent to coxa II, posterior sigilla 1.31 long, 0.57 wide, 1.70 apart, and 1.33 away from sternal margin adjacent to coxa III.

Opisthosoma. Abdomen (Fig. 9A): 14.87 long, 8.30 wide. ovular elongated, integument pale brown. Spinnerets (Fig. 9A): PMS 2.21 long, 0.91 wide, PLS basal segment 3.17 long, 1.65 wide, median segment 1.87 long, 1.33 wide, and apical segment 2.99 long, 1.09 wide.

Genitalia. Spermathecae (Fig. 8C): receptacle 1.40 long, 1.22 wide basally, 0.54 wide distally, lobes 0.31 apart at base. Receptacles unilobed, long, distally converging, apex very narrow, broad basally, apically slightly pointing inward, mesoprolaterally concave, and sclerotized entire.

Legs. Leg formula 4123. Leg lengths total (fem., pat., tib., met., tar.): palp 28.55 (10.55, 5.37, 6.73, n/a, 5.90), leg I 46.34 (13.41, 8.34, 9.76, 8.28, 6.55), leg II 40.23 (11.39, 6.80, 8.82, 8.14, 5.08), leg III 36.49 (9.84, 6.17, 6.80, 8.11, 5.57), leg IV 48.82 (13.56, 6.90, 10.84, 11.95, 5.57). Leg widths (fem., pat., tib., met., tar.): palp (3.32, 2.64, 2.72, n/a, 2.12), leg I (4.08, 3.52, 3.04, 2.20, 2.28), leg II (3.80, 3.00, 2.76, 1.92, 2.00), leg III (3.64, 3.12, 2.80, 2.00, 1.84), leg IV (3.84, 3.32, 3.00, 2.04, 1.88). Tarsi III and IV with transverse weakening (crack or bent), tarsi I and II with no obvious weakening. Spines: Metatarsal spines (dorsal-ventral), met. I 0–1, met. II 0–3,

met. III 2–5 and met. IV 2, 3. Claws: palp with 1 claw, tarsi I–III with pair of claws, tarsus IV with unpaired inferior third claw, all claws have two or three teeth.

Setation. Tactile setae (TS)—carapace entirely with rows of very short yellowish-white TS. Carapace margin, dorsal and upper 1/2 retrolateral surface of chelicerae, ventral prosoma, opisthosoma and legs covered with dark and pale brown, long and short thick TS, longer on leg III, leg IV and abdomen. Mesoprolateral surface of chelicerae with intercheliceral setae in arcuate strip of rows of setae basally spiniform and anteriorly filiform. Above maxillary suture with rows of short spiniform setae, retrolateral surface smooth with vertical striation on distal 1/4 and with rows of fine pallid setae ventrolaterally, and proximal end of prolateral surface with sparse very short spiniform setae. Femoral setation, dense, dark and needleform TS. Scales (SC)—carapace, coxae, trochantera, and femora dorsally with white to pale brown cottony and wavy fine scales, grayish-brown on femora. Chelicerae, dorsal and upper retrolateral surface, dorsal maxilla, sternum, abdomen, dorsal PLS legs, covered with grayish-brown to grayish white lanceolate flat scales, which reflect purplish blue sheen (Fig. 8B), except on ventral abdomen and prolateral femora. Trichobothria—clavate trichobothria present on all leg tarsi, intermixed with epitrichobothria. Clusters of epitrichobothria are present on all tarsi, metatarsi, and tibiae. Filiform trichobothria are present on all dorsal legs, sparsely. Chemosensory sensilla—long and short, pallid and tapering distally, present singly on the entire body except the carapace and chelicerae. Scopulae—palp tar. to tar. III entire, undivided but sparsely intermixed with one or two rows of short stiff setae, one to three rows on tar. III, and tar. IV, entire, divided by four or five rows of long stiff setae; met. I–III, almost entire, undivided but sparsely intermixed with long TS, less sparse on met. III, and met. IV, covering 3/4, divided by two or three rows of long setae and intermixed with long TS.

Color. Bicolored: the legs and opisthosoma are dark, while the carapace, coxae, and trochantera are brown to pale brown dorsally. The microstructures of scales on the legs and abdomen reflect a deep purplish-blue sheen (Fig. 8B). The integument of the carapace is reddish brown. As the exoskeleton aged, the specimen became entirely dark brown before ecdysis.

Indices. CI 80.06, CHI 29.69, CRI 69.02, EI (AME) 3.68, EI (ALE) 4.05, RF 94.92, LI 107.39, TBI 90.04, TI 117.59, SI 44.26.

Etymology. The specific epithet is a noun in apposition, named after the type locality, the Municipality of Libmanan in the Province of Camarines Sur, Philippines.

Orphnaecus tangcongvaca **Acuña & Guevarra, sp. nov.**
https://zoobank.org/63EE9A18-8520-4178-9FF1-04F8B824C2DC
Fig. 9

Orphnaecus sp. "L4" Acuña et al., 2025.

Type material. ***Holotype*** • ♀ PNM 18869 UST-ARC 0142, field# CSL06-02; Philippines: Luzon Island, Bicol Peninsula, Camarines Sur Prov., Libmanan, Brgy. Sigamot, Libmanan Caves National Park; burrows under fallen branch and stones on for-

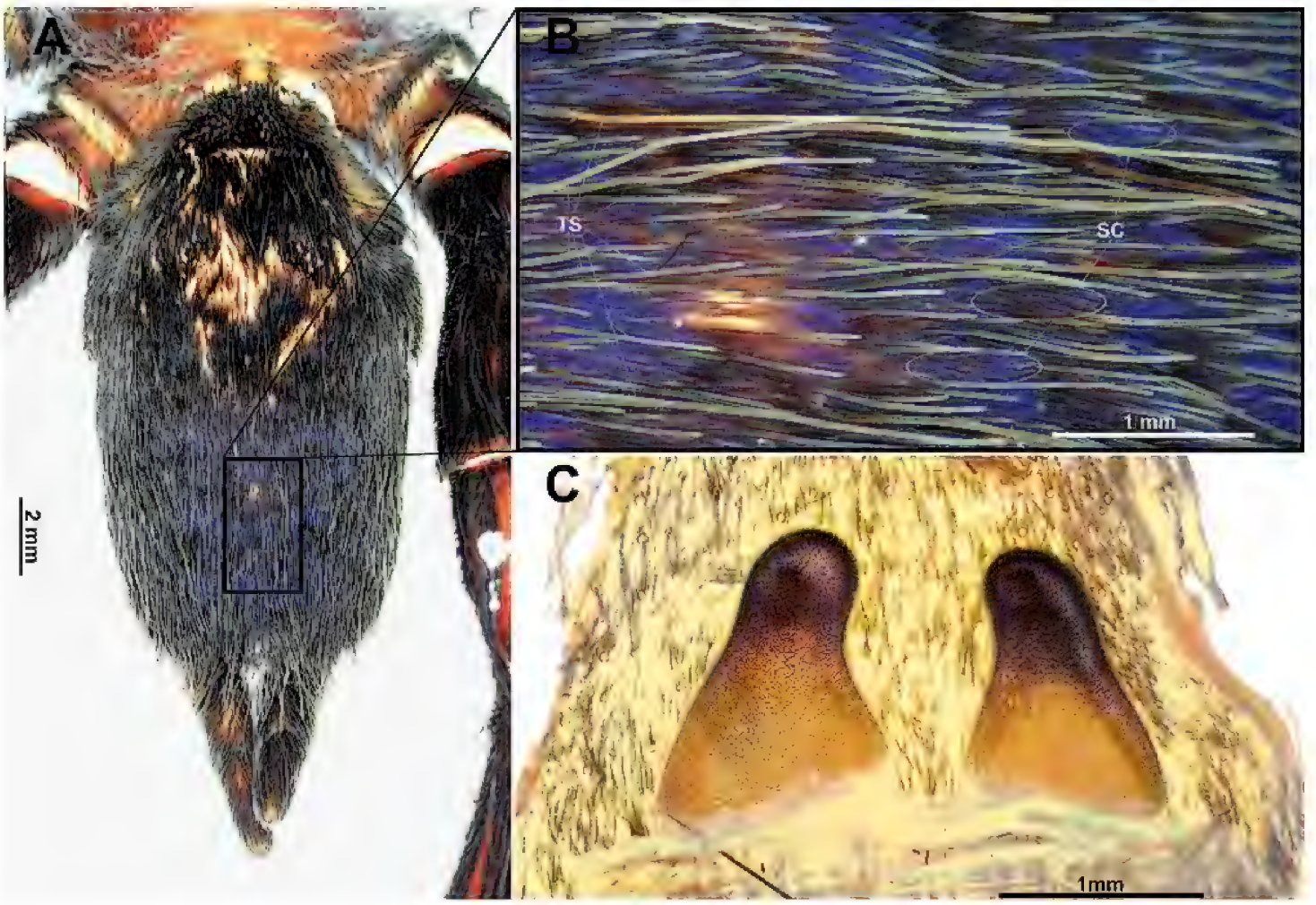

Figure 9. *Orphnaecus libmanan* sp. nov., paratype ♀ opisthosoma and genitalia **A** abdomen, dorsal view **B** magnified view of the setation on the dorsal abdomen showing two types of setae: tactile setae (TS) and scales (SC) **C** spermathecae, dorsal view.

est slope near Laya Cave, 20 July 2023, LA Guevarra, DC Acuña, JD Fornillos leg. ***Paratypes*** • 3♀♀ UST-ARC 0141, 0143, 0144; [same data as for holotype]. (DCA examined).

Type gene sequence. GenBank accession: PP778316 (holotype).

Diagnosis. *O. tangcongvaca* sp. nov. is placed in *Orphnaecus* based on its genetic affinity within the *Orphnaecus* clade and by its spermathecal morphology with lobe converging, slightly pointing inward, and mesoprolaterally concave (Fig. 10J) (Acuña et al. 2025). It is currently the only species that exhibits dwarfism placed in *Orphnaecus* and has dramatically reduced stridulatory organ (lyra) on the prolateral maxilla (Fig. 10H, I). The females further differ from all *Orphnaecus* species (except *O. adamsoni*) by the shape of their female spermathecal lobe, which is broad with its apex slightly narrower than the base but not distinctly narrower than the base (Fig. 10J) with SI ~90 (n = 4) (SI < 65 in all congeners; narrow lobe in *O. pellitus*; distinctly narrower apex than the base in *O. kwebaburdeos* and *O. libmanan* sp. nov., see Acuña et al. 2025, fig. 18). It also differs from *O. libmanan* sp. nov. and *O. pellitus* in having longer tibia I than IV with TBI ~105 (n = 4) (TBI ~90 in the two other species). It further differs in *O. kwebaburdeos* and *O. libmanan* sp. nov. in having shorter tarsus I than IV with TI ~ 91 (n = 4) (TI > 100 in the two other species). It also differs from *O. kwebaburdeos* for having shorter leg I than IV, with RF ~96 (n = 4) in females (I > IV with RF ~101 in *O. kwebaburdeos* female).

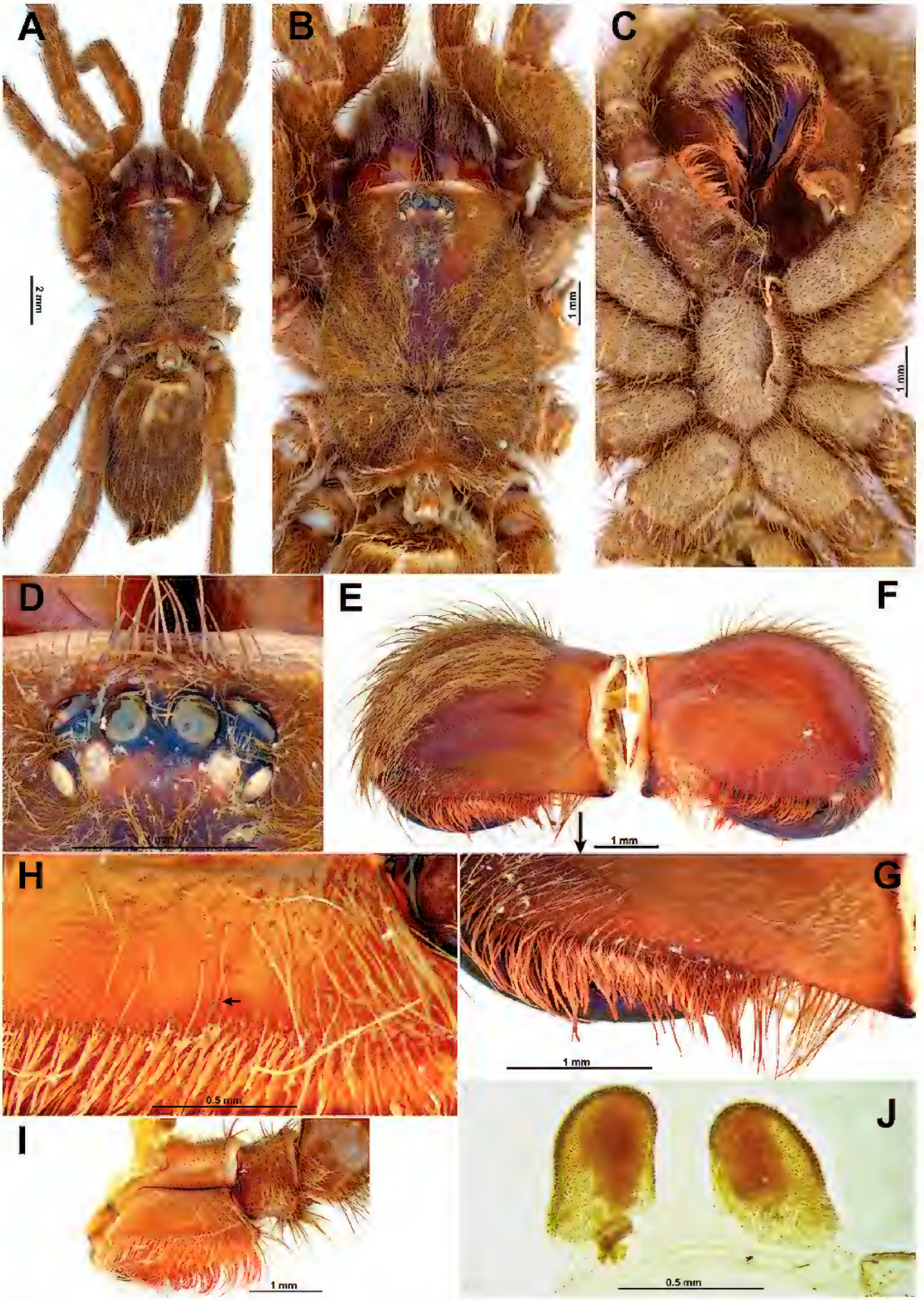

Figure 10. *Orphnaecus tangcongvaca* sp. nov., holotype ♀ **A** habitus, dorsal view **B** prosoma, dorsal view **C** prosoma, ventral view **D** ocular tubercle, dorsal view **E** left chelicera, retrolateral view **F** left chelicera, prolateral view **G** cheliceral strikers at ventrolateral chelicerae **H** left maxilla prolateral surface showing a single stridulatory seta (arrow) **I** left maxilla, prolateral view **J** spermathecae, dorsal view.

Remarks. The male is unknown. *O. tangcongvaca* sp. nov. was not distinguished from the females of *O. adamsoni* since the paratype female is misidentified and misplaced in *Orphnaecus* (see remarks above).

Description. Holotype female, PNM 18869 (UST ARC 0142, field# CSL06-02), body length 16.06. (Fig. 9).

Prosoma. Carapace (Fig. 10B): CL 6.77, CW 4.93, CH 2.00, CR 4.77 long. Ocular tubercle (Fig. 10D): 0.95 long, 1.25 wide. Eyes (Fig. 10D): anterior row slightly procurved at 168°, posterior row recurved at 148°, ALE > AME > PME > PLE, AME 0.33, ALE 0.34, PME 0.32, PLE 0.28. Interocular distances: AME-AME 0.1, ALE-ALE 0.69, PME-PME 0.53, PLE-PLE 0.89, AME-ALE 0.05, AME-PME 0.02, AME-PLE 0.53, ALE-PME 0.24, ALE-PLE 0.14, PME-PLE 0.03. Fovea (Fig. 10B): 0.97 wide, procurved, curvature 131°. Chelicerae (Fig. 10E–G): 3.96 long, 2.80 wide, teeth 10 (nine large, one very small), mesoventral denticles ~28, cheliceral strikers' rows of pallid spiniform setae with filiform ends (Fig. 10G). Maxilla (Fig. 10H, I): 2.23 long, 1.71 wide, maxillary cuspules 187. Lyra (Fig. 10H): composed only of a single short and club-shaped stridulatory seta (Fig. 10H, arrow) (the number could vary when more specimens become available), 0.45 long. Labium: 0.99 long, 1.27 wide, labial cuspules 332, labiosternal sigilla 0.54 long, 0.23 wide, 0.53 apart. Sternum (Fig. 10C): 2.89 long, 1.97 wide, anterior sigilla almost round, 0.17 long, 0.15 wide, 1.49 apart, median sigilla ovoid, 0.28 long, 0.17 wide, 1.63 apart, posterior sigilla ovoid, 0.44 long, 0.17 wide, 1.06 apart.

Opisthosoma. Abdomen (Fig. 10A): 7.52 long, 4.24 wide, ovular elongated. Spinnerets: PMS, 1.00 long, 0.4 wide, PLS, basal segment 1.23 long, 0.55 wide, median segment 0.72 long, 0.6 wide, apical segment 1.16 long, 0.47 wide.

Genitalia. Spermathecae (Fig. 10J): spermathecal lobe 0.52 long, basal width 0.39, distal width 0.35, basally 0.20 apart, unilobed, distally slightly converging, apically slightly pointing inwards, and concave mesoprolaterally.

Legs. Leg formula 4123. Leg lengths (fem., pat., tib., met., tar.): palp 10.56 (3.58, 2.08, 2.52, n/a, 2.38), leg I 16.48 (4.8, 2.72, 4.08, 2.8, 2.08), leg II 14.32 (4.08, 2.48, 3.12, 2.56, 2.08), leg III 11.72 (3.52, 1.56, 2.16, 2.52, 1.96), leg IV 17.12 (5.00, 2.04, 3.88, 3.92, 2.28). Leg widths (fem., pat., tib., met., tar.): palp (1.42, 1.04, 1, n/a, 0.78), leg I (1.64, 1.28, 1.2, 0.88, 0.76), leg II (1.48, 1.2, 1.04, 0.84, 0.64), leg III (1.33, 1.12, 0.88, 0.72, 0.6), leg IV (1.36, 1.16, 1, 0.72, 0.6). Coxae (Fig. 10C): (palpcoxa, see Prosoma:Maxilla) Length (coxa I–IV) 2.93, 2.13, 1.87, 2.21. Width (coxa I–IV) 1.33, 1.31, 1.33, 1.44. Trochantera: Length (troch. palp–IV) 0.79, 1.44, 1.31, 1.1, 1.09. Width (troch. palp, I–IV) 1.29, 1.25, 1.15, 1.12, 1.47. Tarsi III and IV with transverse weakening (cracked or bent), tarsi I and II with no visible weakening. Spines: Metatarsal spines (dorsal-ventral), met. I 0–1, met. II 0–3, met. III 2, 3, met. IV. 2, 3. Claws: palp with one claw, tarsi I–III with pair of claws, tarsus IV with unpaired inferior third claw, all claws have no teeth.

Setation. Tactile setae (TS)—brown to pale brown, pallid apically, strong TS covering body and legs, dense on ventral tibia I. Dark spiniform and translucent setae present on all lateral coxae. Femoral setation on femur I sparsely covered with fine needleform setae, intermixed with scales. Scales (SC)—lanceolate SC, reflect-

ing pale brown color, covering all legs, sternum, chelicerae, and spinnerets brown on the entire abdomen. Cottony pale brown SC covering the carapace. Trichobothria—clavate trichobothria present on all tarsi, intermixed with epitrichobothria. Clusters of epitrichobothria are present on all metatarsi, tarsi, and tibiae. Filiform trichobothria are present sparsely on all dorsal legs. Filiform trichobothria present on all dorsal legs, sparsely. Chemosensory sensilla—short, translucent, tapering distally, present singly on the entire body except the carapace and chelicerae. Scopulae—tarsal palp, entire, divided by one or two rows of stiff setae; tar. I, entire, divided by two or three rows of stiff setae; tar. II, entire, divided by two or three rows of stiff setae; tar. III, entire, divided by two or three rows of stiff setae; tar. IV, entire, divided by rows of stiff setae; met. I, almost entire, divided by a row of very sparse long setae; met. II, almost entire, divided by a row of very sparse long setae; met. III, covering 3/5, divided by one or two rows of very sparse long setae; met. IV, covering half, divided by two or three rows of sparse long setae.

Color. Entirely uniform brown clothed with brownish setation (Fig. 10A).

Indices. CI 72.82, CHI 29.54, CRI 70.46, EI (AME) 4.88, EI (ALE) 5.02, RF 96.26, LI 119.01, TBI 105.16, TI 91.23, SI 89.74.

Male. Unknown. An adult dwarf male was found under the same fallen branch as the holotype female, but managed to escape on the vegetation.

Etymology. The specific epithet is a noun in apposition in honor of the Tangcong Vaca Guerilla Unit, founded in Camarines Sur and established its base at Tangcong Vaca mountain in Libmanan during the Japanese occupation of the Philippines.

Distribution, ecology and niche partitioning

Culapnitan Caves, a cave system currently located within the Libmanan Caves National Park (LCNP), is the known type locality of *O. pellitus*. LCNP is located 350 km south of the capital city, Manila, in the Municipality of Libmanan, Province of Camarines Sur (Fig. 11). Based on the sampling location profile, *O. pellitus* was exclusively collected inside the interconnected caves of Alinsanay, Kalangkawan, and Laya which suggests that *O. pellitus* is a troglobiont.

O. pellitus is found starting at ~30 m horizontal depth from the cave entrance, where no natural light penetrates owing to the almost vertical cave entrance and the shade from the forest canopy. The horizontal burrows are found in piles of dry and damp guano substrates on the cave floors, often under limestone rocks (Fig. 12E–G). The burrows were shallow (up to 15 cm deep) and lined with silk mats. They were observed to feed on Rhaphidophoridae, which are abundant on cave floors. They likely preyed on other arthropods found within the caves, but no observations have been recorded thus far. Their natural predators are unknown, although a potential predator, the invasive toad *Rhinella marina*, is found inside the Alinsanay Cave near the cave entrance. All the life stages were found within the cave system. No conspecifics were found outside and at the immediate entrance of the caves after an extensive search. Fig. 12 shows the habitat of *O. pellitus* and the ecology inside the Alinsanay, Kalangkawan, and Laya Caves.

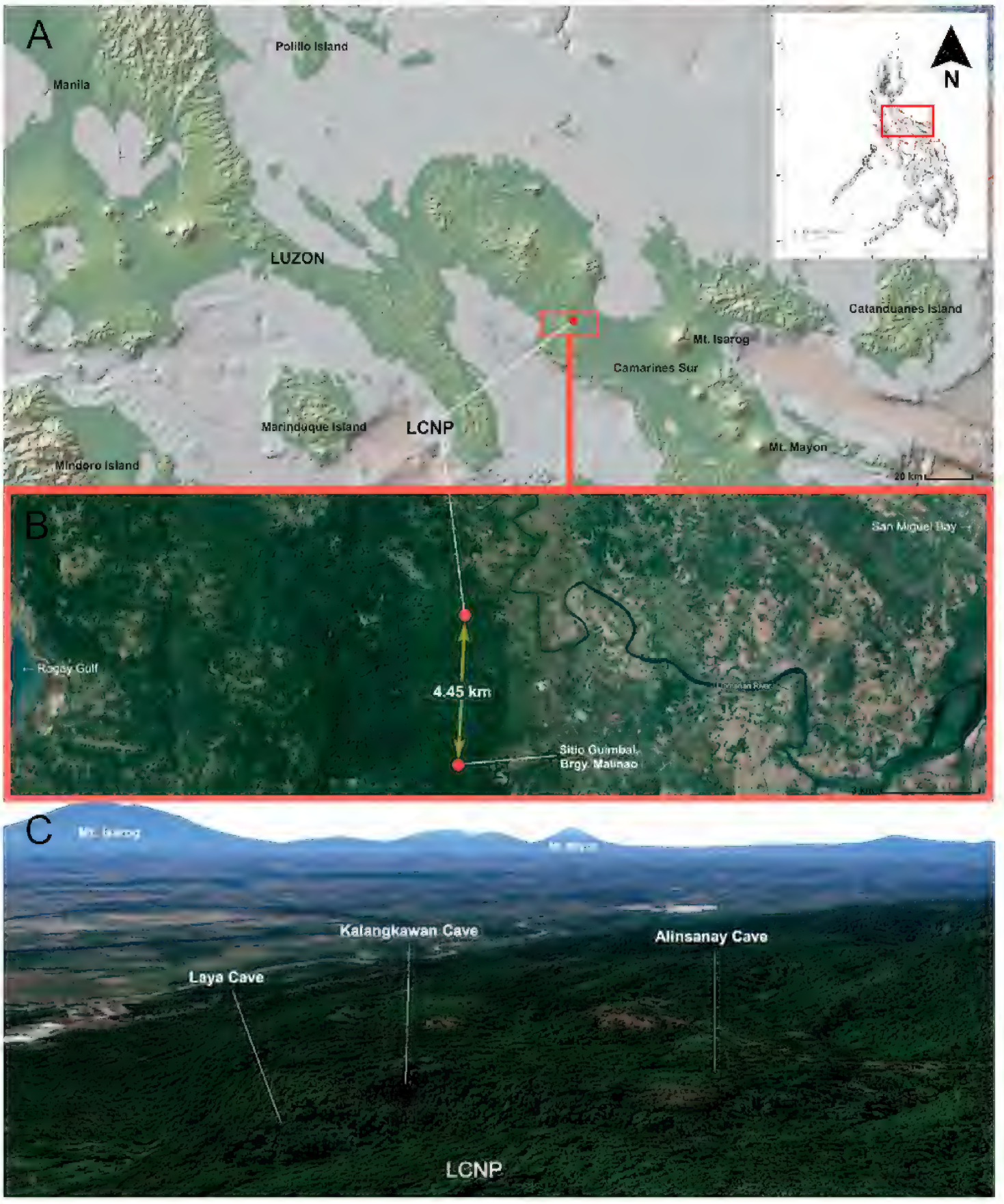

Figure 11. Map of the collection sites in Libmanan, Camarines Sur Province **A** Libmanan Caves National Park (LCNP), Brgy. Sigamot, Libmanan, Camarines Sur **B** type localities of *O. libmanan* sp. nov. in LCNP and Sitio Guimbal, Brgy. Malinao, Libmanan, Camarines Sur **C** aerial view of LCNP with the cave entrances of Culapnitan Caves system. Map: Bathymetry © 2024 GMRT; Satellite and aerial map © 2024 Google.

Aside from *O. pellitus*, which is exclusively found inside caves, *O. libmanan* sp. nov. and *O. tangcongvaca* sp. nov. are also cohabitants of LCNP. Both species were found outside the lowland forests of the protected area (Fig. 13A–F). We were also able to record the presence and collect samples of *O. libmanan* sp. nov. some 4.5 km from the LCNP in Sitio Guimbal, Barangay Malinao of the Municipality of Libmanan.

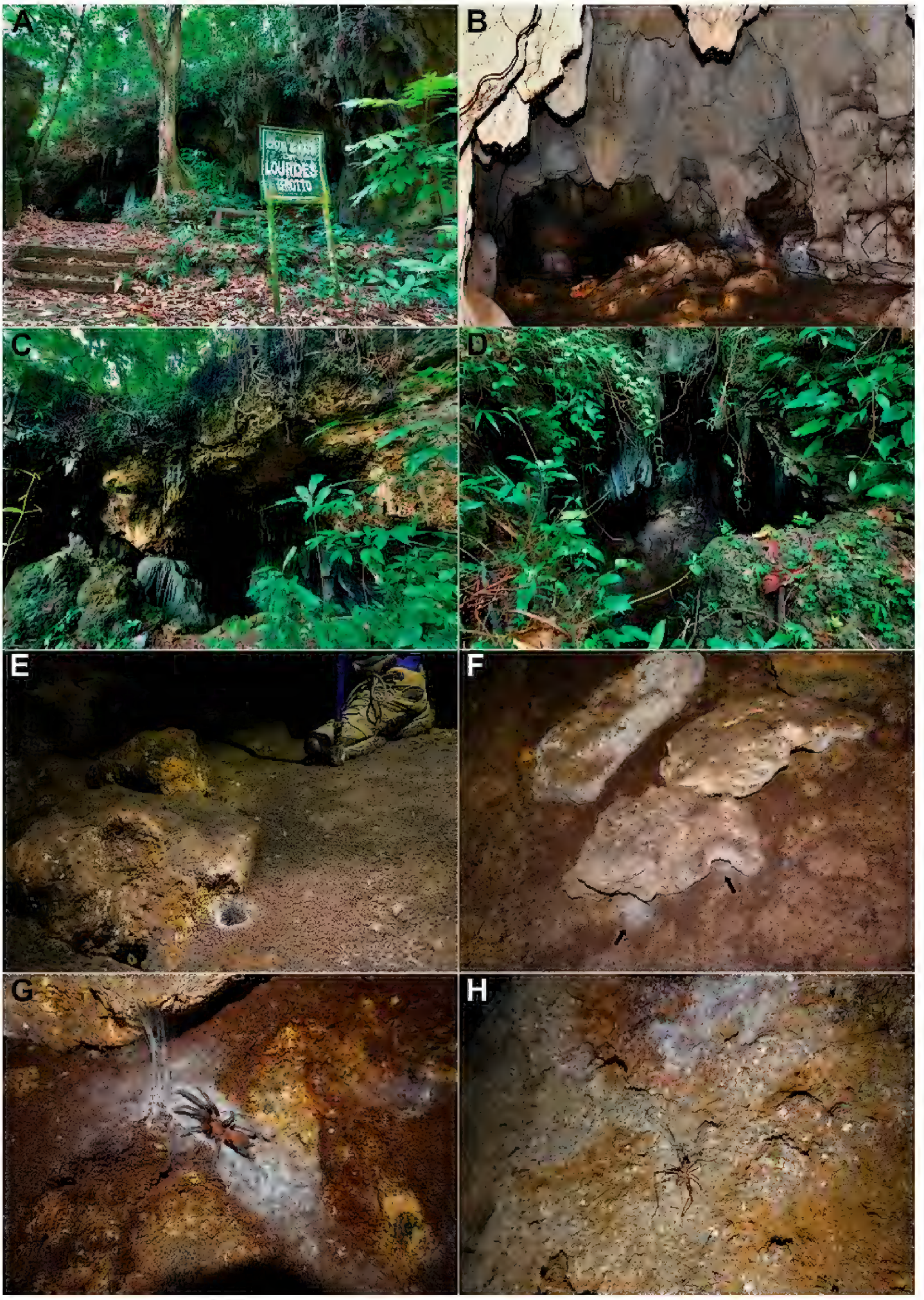

Figure 12. Habitat of *Orphnaecus pellitus* in LCNP in the Municipality of Libmanan, Camarines Sur Province **A** Kalangkawan Cave entrance **B** internal structure of Kalangkawan Cave **C** Laya Cave entrance **D** Alinsanay Cave entrance **E** burrow entrance of *O. pellitus* under limestone rock in Kalangkawan Cave **F** burrow entrances (arrows) of *O. pellitus* under a limestone rock in Laya Cave **G** *O. pellitus*, in situ, in its simple horizontal burrow laid with silk mat under a flipped limestone rock in Laya Cave **H** a cave cricket, Rhaphidophoridae, inside Laya Cave, the primary prey of *O. pellitus*.

Figure 13. Habitat of the two new epigean *Orphnaecus* species in LCNP (**A–F**) and Brgy. Malinao (G, H), in the Municipality of Libmanan, Camarines Sur Province **A** forest slope in LCNP adjacent to Kalangkawan Cave, with the authors (DCA and LAG) and a field assistant (JD Fornillos) during the field sampling in April **B** burrow of *O. libmanan* sp. nov. above ground on the crevices of the roots of a tree attached to a limestone formation, found in July (DCA in frame) **C** *O. libmanan* sp. nov., paratype female, in its burrow in the core of a fallen log **D** arrow pointing the burrow entrance of the same fallen log before extraction of the specimen **E** *O. tangcongvaca* sp. nov., holotype female, in situ, adjacent to Laya Cave **F** *O. tangcongvaca* sp. nov., paratype female, in situ, in its horizontal burrow under a decaying branch **G** *O. libmanan* sp. nov. habitat in Brgy. Malinao with burrows found under piles of coconut husks **H** *O. libmanan* sp. nov. burrow entrance under a limestone rock on a stream bank in Brgy. Malinao.

O. libmanan sp. nov. is a typical epigean species found in their horizontal burrows under and inside large dead logs (Fig. 13C, D) and under a large limestone rock (Fig. 13H). They were also found inside piles of coconut husks on the forest floor (Fig. 13G) during the wet season in July, but absent on the same piles during the initial sampling in the dry season in April. One specimen was found in a burrow inside a tree hole more than a meter above the ground in July (Fig. 13B, arrow), which was probably displaced from the ground owing to flooding in the rainy season.

O. tangcongvaca sp. nov., on the other hand, is known only from the type locality on the forest floor of LCNP. This dwarf epigean species was found in the horizontal burrows under fallen tree branches (Fig. 13F), and stones on the forest floor covered with thick vegetation and leaf litter. An adult male was observed during the wet season in July (uncollected). This species is sympatric with *O. libmanan* sp. nov. but potentially occupies a different niche, probably preying limitedly on smaller arthropods that are out of the diet preferences of *O. libmanan* sp. nov. and burrowing on smaller spaces under litter, fallen branches, and stones, avoiding direct competition for food and space.

The successful coexistence and occurrence of the three species of *Orphnaecus* in the LCNP can be explained by the differentiation of their habitat (Fig. 14) and the ecological roles (realised niche) of each species in its environment, shaped by both their potential role (fundamental niche) and the limitations imposed by biotic and abiotic factors.

The habitat of the troglobiont, *O. pellitus*, can be distinguished from that of its congeners in the LCNP by its exclusive colonisation of the cave floor in the Culapnitan Cave system. *O. pellitus* is observed to predate on an unidentified cave cricket species (Rhaphidophoridae), which is abundant on the floors of the explored caves. However, two epigean species, *O. tangcongvaca* sp. nov. and *O. libmanan* sp. nov., coexist on the forest floor of the LCNP. The second speciation event in LCNP is the divergence and dwarfism of *O. tangcongvaca* sp. nov. Termite carcasses were found in their burrows which is potentially out of the preference of most *O. libmanan* sp. nov. Overlaps in food and space may exist between the two sympatric species (as shown in Fig. 14), but could be minimal, possibly because the spiderlings of *O. libmanan* compete with *O. tangcongvaca*. It was also observed that *O. tangcongvaca* burrows under stones and fallen branches on the ground, which deviates from the large burrows of *O. libmanan*, which require larger ground covered by logs and large rocks (as illustrated in Fig. 14). *O. libmanan* burrows were found inside the hollow core of fallen logs, under large limestone rocks, in holes of a living tree (>1 m above ground during the wet season), and inside piles of coconut husks.

Discussion

Morphological and phylogenetic analyses, as well as ecological differentiation of the spiders collected in the LCNP and adjacent communities, resulted in the identification of three tarantula species, one from inside the caves and two from outside. The specimen collected from the cave was morphologically confirmed to be *O. pellitus* by examination of the syntypes, whereas the specimens collected

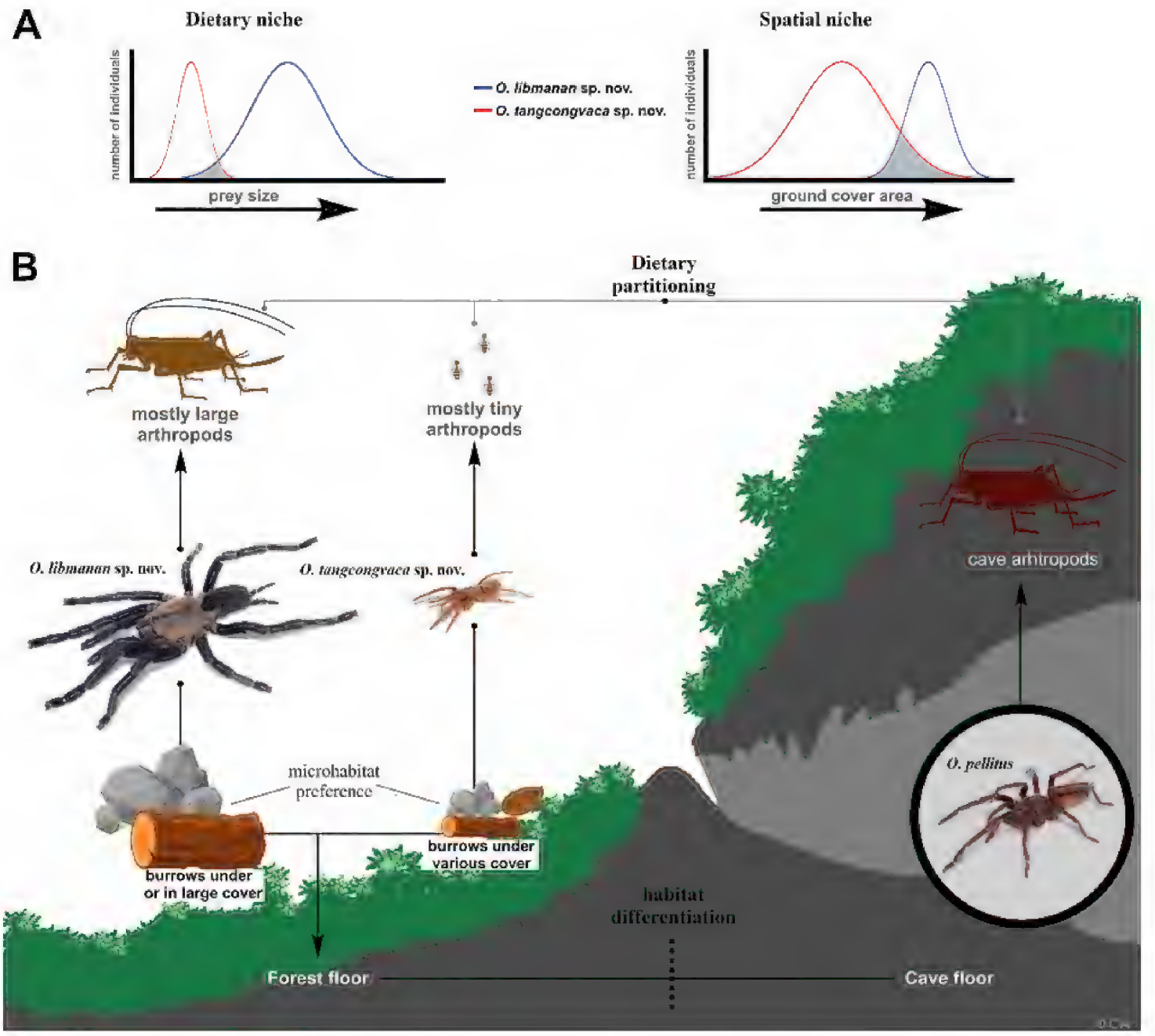

Figure 14. Ecological niche structure of the theraphosid species of LCNP **A** hypothetical distribution curve of dietary niche based on the size of prey and spatial niche based on the area of microhabitat ground cover between the sympatric species, *O. libmanan* sp. nov. and *O. tangcongvaca* sp. nov. **B** niche partitioning model among the tarantula species in LCNP. *O. pellitus* exclusively inhabits the cave floors in LCNP, which preys on cave-dwelling insects such as the cave crickets (Rhaphidophoridae). In contrast, *O. libmanan* sp. nov. and the dwarf *O. tangcongvaca* sp. nov. are sympatric species dwelling on the forest floors of LCNP but mostly occupy different microhabitats and diet preferences, avoiding direct competition for space and food resources.

outside, one typical-sized tarantula and one dwarf, did not conform to any of the described Philippine tarantula species. *O. pellitus* was exclusively collected from the inside of the cave. At the same time, the other two new species, *O. libmanan* sp. nov. and *O. tangcongvaca* sp. nov., were exclusively collected outside (the nearest is approximately 10 m from the cave opening).

Recognition of troglobitic species is challenging and, in most cases, requires physical strength and expertise in cave exploration. While cave biodiversity surveys started in the mid-1900s, it was only in the 1960s that most troglobitic species were recognised because of the previously accepted paradigm that troglobites do not exist

in temperate limestone caves. Early explorers also had almost no experience recognising troglomorphic characteristics, as this concept gained popularity only in the 1980s (Howarth 2022).

In a recent investigation performed on new specimens of *O. pellitus* collected inside the cave, notable troglomorphic characteristics, such as reduction in eye size, reduction in tactile setae length, attenuation of limb size, and diminishing pigmentation, were observed. Reduction in size or complete absence of the eyes is the most common observable feature among troglobionts because the eyes become non-functional and vestigial organs in the absence of light (Friedrich 2013; Deharveng and Bedos 2018). This may explain why the measured diameter of ALE of *O. pellitus* is significantly smaller than that compared to its congeners, also suggesting that tarantula's ALEs are essential in the visual behaviour of spiders like what was observed in Lycosidae (Ortega-Escobar and Ruiz 2017). In addition to the reduction in eye size, the dark environment in the cave also made colouration less critical; hence, the observed reduction in pigmentation of troglobitic organisms (Vargovitsh 2017). Morphological and physiological characteristics may also change owing to environmental stress. The observed attenuation of the legs of *O. pellitus* could be an adaptation to the limited nutrient sources in the cave environment. This adaptation, which includes regulation of the growth of body parts, has been observed in both invertebrates and vertebrates owing to conserved signalling pathways that regulate growth in animals (Koyama and Mirth 2018). In addition, the shorter tactile setae of *O. pellitus* may also be attributed to lesser activity in the caves' enclosed environment. Tactile setae are the most common sensilla of tarantulas covering the body and limbs, and their primary function is the perception of physical touch (Guadanucci 2020). Owing to the fewer activities, disturbances, and obstacles inside the cave, tactile setae seldom became functional; hence, this sensing organ became shorter.

Tolerance to hypoxia, increased sensitivity to movements, and better predation drive are evolutionary adaptations observed in cave-dwelling tarantula. Subterranean environments putatively have lower oxygen levels than surface environments (Hervant and Malard 2019). This suggests that *O. pellitus* has adapted to one of the subterranean environment pressures with high tolerance to oxygen levels (lower than atmospheric concentrations) inside the cave system. Greater predation drive may be attributed to more opportunistic prey capture and greater sensory in an environment with limited nutrient and energy resources. In subterranean environments, organisms rely on mechano-sensitive sensilla, such as trichobothria, to detect mechanical vibrations, compensating for the ineffectiveness of vision in lightless conditions (Reissland and Görner 1985; Partha et al. 2017; Rebora et al. 2019). There are three types of trichobothria on tarantulas: filiform, thickened, and clavate. Air currents are detected by the filiform trichobothria by its very thin, pale, and erect sensilla that are found on the dorsal and lateral tibia, metatarsus, and tarsus, which can easily be moved by air movement. Another type is the clavate trichobothria, which are found on the dorsal tarsus forming two parallel rows and are sensitive to ground vibrations due to their structure with

large clavate apical ends and thin base inserted into cup-shaped bothrium. They can be easily disturbed by the slightest movement from the ground. However, our morphological analysis did not reveal any mutations in the structure or increase in the number of trichobothria (Guadanucci 2012, 2020). It is presumed that the enhanced response to stimuli developed internally through its neurological processes.

The lyrate, cheliceral, and genital morphology of the typical-sized tarantula collected outside the cave, *O. libmanan* sp. nov., corresponds to that of an *Orphnaecus*, hence its placement. This is supported by phylogenetic analysis, wherein the regular-sized tarantula, *O. libmanan* sp. nov., is in the *Orphnaecus* clade. As described above, its morphological differences and genetic divergence from its congeners support its distinction as a new species, with *O. kwebaburdeos* as the nearest genetic relative.

Dwarf tarantulas in the Philippines are currently placed in the genus *Phlogiellus* Pocock, 1897, a 'wastebasket' genus for most dwarf selenocosmiine species with rudimentary or absent lyra. However, phylogenetic analysis of the dwarf species collected from LCNP, *O. tangcongvaca* sp. nov., suggests that it belongs to the genus *Orphnaecus* and not within a separate clade. Our classification of this dwarf species may raise issues, especially for those who have reservations on the reliability of molecular taxonomy, however, disregarding phylogenetic observations and placing all selenocosmiine species with plastic and weak characters such as dwarfism and the reduction or loss on lyra solely to *Phlogiellus* (as proposed by Raven 2005), can threaten the future of morphology-based cladistics (Jenner 2004; Sereno 2009). Incongruence between morphology and molecular phylogeny has also been observed in Theraphosinae with high degrees of homoplasy (Ortiz et al. 2018). We considered dwarfism and reduction or loss of lyra homoplastic characteristics within Selenocosmiinae, which means that they can occur in all included genera. Hence, with the doubt of monophyly of *Phlogiellus*, other junior synonyms of the genus such as *Yamia* Kishida, 1920 and *Baccalbrapo* Barrion & Litsinger, 1995, might need to be reexamined and resolved with the help of molecular phylogenetic approach. The synonymy of *Neochilobrachys* Hirst 1909 (a dwarf genus with reduced lyra) to *Chilobrachys* Karsch, 1892 by Nunn et al. (2016) seems to be valid (rather than to *Phlogiellus*, as proposed by Raven 1985), as this could be the dwarf version of the genus due to their synapomorphy as described by Hirst (1909) and Nunn et al. (2016). Furthermore, West et al. (2012) mentioned that there are undescribed *Orphnaecus* species with absent maxillary lyra, and our phylogenetic results evidently placed *O. tangcongvaca* sp. nov., a dwarf with almost absent lyra, within the *Orphnaecus* clade. The spermathecal shape of female *O. tangcongvaca* sp. nov. also fits with the spermathecal morphology of *Orphnaecus*, in contrast to *Phlogiellus*, which usually has apically swollen spermathecae (Nunn et al. 2016). The maxillary lyra of *O. tangcongvaca* is an extremely reduced version of the typical morphology of *Orphnaecus*, retaining only a single club-shaped bacillae; however, the reduction and number of lyra could vary when more specimens become available.

The genetic divergence of *O. pellitus* from the epigean species of LCNP, *O. libmanan* sp. nov. and *O. tangcongvaca* sp. nov., suggests that *O. pellitus* is dis-

tantly related to the two species living outside the cave. This intriguing finding may suggest ancient diversification, possibly inter-geologic period migration, among tarantula species in the Philippines or possibly in Southeast Asia due to glaciation period climactic adaptation and migration, which has been observed in arthropods and arachnids including spiders and scorpions (Sharma et al. 2018; Chen et al. 2020; Li et al. 2020). However, this requires further study and the inclusion of more species, especially from karst and forest environments, which became a refuge for living organisms, including troglophilic spiders during the Pleistocene and Miocene periods (Morgan et al. 2010; Ballarin and Li 2018; Bacon et al. 2021). In TimeTree COI dating, we followed the time estimates of Foley et al. (2021) for the age of Theraphosidae. Biswas et al. (2023) have also estimated the age of Theraphosidae but have a younger age estimate. This is possibly due to the different distribution mathematical models used and maybe due to their placement of the Burmese amber fossil, Protertheraphosinae (~100 Ma), for time calibration as the oldest node for the Theraphosidae clade. However, Protertheraphosinae could be the direct ancestor of Selenocosmiinae and Thrigmopoeinae based on the morphological description of the *Protertheraphosa spinipes* Wunderlich & Müller, 2020 which have potential synapomorphy (e.g. lack of tibial apophysis/spur in males) with this Asian clade (Wunderlich and Müller 2020). In addition, the age estimate for the Selenocosmiinae-Theraphosinae split in Foley et al. (2021) is 106.5–111 Ma which is close to the approximate age of the Burmese amber fossil (~100 Ma).

The ecological dynamics of the LCNP may have promoted divergence over time. Competition for resources may have forced some ancient populations to explore new resources and habitats. The colonisation of caves by *O. pellitus* may be driven by the opportunity to occupy new and unexploited habitats brought about by climatic conditions or competition pressure on space and food resources from its former epigean conspecifics, as emphasised by the active colonisation theory (adaptive shift hypothesis) (Howarth 1980; Rouch and Danielpol 1987). The hypogean conditions of the cave created island-like isolation, eventually leading to genetic divergence through parapatric speciation, which explains the absence of conspecifics outside the cave at present. The dwarfism of *O. tangcongvaca* sp. nov. is likely due to competition for space and food resources. Competition pressure on prey could have led this species to shift to smaller insects, such as the termites herein observed, that are out of the preference of its former conspecific and may have caused the decrease in body size; hence, sympatric speciation became possible. Dwarfism also shifted the microhabitat requirement of this species, thus lessening competition for space, as observed where the burrows are found. The occurrence of small and large species in a genus was also observed in *Aphonopelma* Pocock, 1901, with the *paloma* species group comprising relatively small-sized species typically found in barren habitats such as deserts, grasslands, and shrublands (chaparral) (Hamilton et al. 2016). Ancestors of *O. libmanan* sp. nov. may have continued to spread from most of southern Luzon and southward to Mindanao with multiple divergences occurring possibly due to geological dynamics, such

as island fragmentation, as revealed in the divergence of the *Orphnaecus* sp. from Mindanao and the recent genetic split of the mainland species, *O. libmanan* sp. nov. and the island-endemic, *O. kwebaburdeos*.

Conclusion

The theraphosid species assemblage of LCNP is composed of at least one genus and three species that belong to the subfamily Selenocosmiinae—*Orphnaecus pellitus*, *Orphnaecus libmanan* sp. nov., and *Orphnaecus tangcongvaca* sp. nov. The hypogean *O. pellitus* inhabits some of the interconnected caves of the Culapnitan Cave system in LCNP, while the two epigean species sympatrically inhabit the adjacent forest floors but occupy different ecological niches. Greater conservation efforts and more biodiversity surveys are recommended for the LCNP, especially for its unexplored caves that might harbour other unique species with interesting subterranean biology waiting to be discovered. The theraphosid diversity of the Philippines has now increased to 16 species (all are endemic).

We recognised 19 known troglobitic tarantula species in the world, with most from the Americas and one species from Asia (Table 3). The rediscovery of *O. pellitus* led us to the conclusion that it is a true troglobiont, as evident in its troglomorphism and subterranean adaptations, which is the first published troglobitic tarantula species in Asia and the world (Simon, 1892). The discovery of more troglobitic species is expected in other parts of Asia, based on its subterranean ecosystems. Molecular phylogenetic studies are necessary to resolve problematic taxa in Selenocosmiinae, particularly those with homoplasy, such as dwarf species currently in the genus *Phlogiellus*.

Table 3. Updated list of troglobitic tarantula species worldwide and their known distributions.

	Troglobitic theraphosid species	Distribution
Americas		
1.	*Hemirrhagus stygius* (Gertsch 1971)	Mexico (Cueva de los Potrerillos and Sótano del Pozo)
2.	*H. puebla* (Gertsch 1982)	Mexico (Cueva de Tasalolpan)
3.	*H. reddellli* (Gertsch 1973)	Mexico (Cueva del Nacimiento del Río San Antonio)
4.	*H. grieta* (Gertsch 1982)	Mexico (Cueva de la Grieta)
5.	*H. mitchelli* (Gertsch 1982)	Mexico (Entrada del Viento Alto)
6.	*H. elliotti* (Gertsch 1973)	Mexico (Cueva de la Laguna)
7.	*H. gertschi* Pérez-Miles & Locht, 2003	Mexico (Resumidero)
8.	*H. coztic* Pérez-Miles & Locht, 2003	Mexico (Cueva de San Juan)
9.	*H. ocellatus* Pérez-Miles & Locht, 2003	Mexico (Cueva de la Peña Blanca)
10.	*H. papalotl* Pérez-Miles & Locht, 2003	Mexico (Gruta de Aguacachil/Zacatecolotla)
11.	*H. akheronteus* Mendoza & Francke, 2018	Mexico (Cueva del Río Jalpan)
12.	*H. billsteelei* Mendoza & Francke, 2018	Mexico (Cueva de la Grieta)
13.	*H. diablo* Mendoza & Francke, 2018	Mexico (Cueva del Diablo)
14.	*H. kalebi* Mendoza & Francke, 2018	Mexico (Cueva de las Abejas)
15.	*H. sprousei* Mendoza & Francke, 2018	Mexico (Cueva de la Laguna Verde)
16.	*H. valdezi* Mendoza, 2014	Mexico (Cueva Redonda)
17.	*Holothele maddeni* (Esposito & Agnarsson, 2014)	Dominican Republic (Cueva Seibo)
18.	*Tmesiphantes hypogeus* Bertani et al., 2013	Brazil (Gruna das Cobras and Gruna da Parede Vermelha)
Asia		
19.	*O. pellitus* Simon, 1892 (this study)	Philippines (Culapnitan Caves/ Libmanan Caves National Park)

Acknowledgments

We thank the Philippines Department of Science and Technology (DOST) and the National Research Council of the Philippines (NRCP) for funding the GAGAMBA Research Program. The Department of Environment and Natural Resources-Biodiversity Management Bureau (DENR-BMB), Department of Environment and Natural Resources Region 5, Libmanan Caves National Park - Protected Areas Management Bureau (LCNP-PAMB), and the Municipality of Libmanan for issuing necessary research permits and consents. The authors also thank Ms. Eilisse-Anne Leguin (MNHN), and Dr. Christine Rolland and Mr. Boris Striffler (Germany) for the opportunity to examine the syntypes of *O. pellitus*; to the UPLB-MNH for the opportunity to examine the types of *O. kwebaburdeos*; to Mr. Perry Buenavente of the PNM for the opportunity to examine the types of *O. adamsoni*. Ms. Maria Mikaela Dumbrique of the University of Santo Tomas for performing the extraction of DNA used in this study; Mr. Charles Nylxon Noriega of the University of the Philippines-Diliman, Mr. John Denver Fornillos of Laguna State Polytechnic University - Sta. Cruz campus, and the staff of LCNP-PAMB for their assistance during the field sampling in LCNP.

References

Acuña DC, Dumbrique MMU, Ranido MC, Ragasa LP, Noriega CNC, Mayor ABR, Florendo Jr GA, Fadri MJA, von Wirth V, Santiago-Bautista MR, Guevarra Jr LA (2025) Taxonomic revalidation of *Selenobrachys* Schmidt, 1999 and *Chilocosmia* Schmidt & von Wirth, 1992 based on morphological and molecular analyses (Araneae, Theraphosidae), with the description of a new species from Romblon Island, Philippines. ZooKeys 1233: 139–193. https://doi.org/10.3897/zookeys.1233.128056

Bacon AM, Bourgon N, Welker F, Cappellini E, Fiorillo D, Tombret O, Thi Mai Huong N, Anh Tuan N, Sayavonkhamdy T, Souksavatdy V, Sichanthongtip P, Antoine PO, Duringer P, Ponche JL, Westaway K, Joannes-Boyau R, Boesch Q, Suzzoni E, Frangeul S, Patole-Edoumba E, Zachwieja A, Shackelford L, Demeter F, Hublin JJ, Dufour É (2021) A multiproxy approach to exploring *Homo sapiens*' arrival, environments, and adaptations in Southeast Asia. Scientific Reports 11(1): 21080. https://doi.org/10.1038/s41598-021-99931-4

Ballarin F, Li S (2018) Diversification in tropics and subtropics following the mid-Miocene climate change: A case study of the spider genus *Nesticella*. Global Change Biology 24(2): e577–e591. https://doi.org/10.1111/gcb.13958

Barrion-Dupo AL, Barrion A, Rasalan J (2015) A new cave-dwelling mygalomorph spider of the genus *Phlogiellus* Pocock, 1897 (Araneae: Theraposidae: Selenocosmiinae) from Burdeos, Polilio Island, Quezon Province, Philippines. Philippine Journal of Systematic Biology 8: 1–15.

Behrmann-Godel J, Nolte AW, Kreiselmaier J, Berka R, Freyhof J (2017) The first European cave fish. Current Biology 27(7): R257–R258. https://doi.org/10.1016/j.cub.2017.02.048

Bertani R (2009) Male palpal bulbs and homologous features in Theraphosinae (Araneae, Theraphosidae). Journal of Arachnology. 28: 29–42. https://doi.org/10.1636/0161-8202(2000)028[0029:MPBAHF]2.0.CO;2

Bertani R, Bichuette ME, Pedroso DR (2013) *Tmesiphantes hypogeus* sp. nov. (Araneae, Theraphosidae) is Brazil's first troglobitic tarantula. Anais da Academia Brasileira de Ciências 85: 235–243. https://doi.org/10.1590/s0001-37652013005000007

Biswas A, Chaitanya R, Karanth KP (2023) The tangled biogeographic history of tarantulas: An African centre of origin rules out the centrifugal model of speciation. Journal of Biogeography 00: 1–11. https://doi.org/10.1111/jbi.14678

Bloom T, Binford G, Esposito LA, Garcia GA, Peterson I, Nishida A, Loubet-Senear K, Agnarsson I (2014) Discovery of two new species of eyeless spiders within a single Hispaniola cave. The Journal of Arachnology 42:148–154. https://doi.org/10.1636/K13-84.1

Bryant D, Moulton V (2004) Neighbor-Net: An agglomerative method for the construction of phylogenetic networks. Molecular Biology and Evolution 21(2): 255–265. https://doi.org/10.1093/molbev/msh018

Chen L, Sun JT, Jin PY, Hoffmann AA, Bing XL, Zhao DS, Xue XF, Hong XY (2020) Population genomic data in spider mites point to a role for local adaptation in shaping range shifts. Evolutionary Applications 13(10): 2821–2835. https://doi.org/10.1111/eva.13086

Clements R, Sodhi N, Schiilthuizen M, Ng P (2006) Limestone karsts of Southeast Asia: Imperiled arks of biodiversity. Bioscience 56:733–642. https://doi.org/10.1641/0006-3568(2006)56[733:LKOSAI]2.0.CO;2

Culver DC, Pipan T (2009) The Biology of Caves and Other Subterranean Habitats. Oxford University Press, New York, 272 pp.

de Souza PE, Souza-Silva M, Ferreira RL (2024) The ticking clock in the dark: Review of biological rhythms in cave invertebrates. Chronobiology International 41(5): 738–756. https://doi.org/10.1080/07420528.2024.23480

Deharveng L, Bedos A (2012) Diversity Patterns in the Tropics. Encyclopedia of Caves, 238–250. https://doi.org/10.1016/b978-0-12-383832-2.00032-3

Deharveng L, Bedos A (2018) Diversity of Terrestrial Invertebrates in Subterranean Habitats. Ecological Studies 235: 107–172. https://doi.org/10.1007/978-3-319-98852-8_7

de Queiroz K (2005) A Unified Concept of Species and Its Consequences for the Future of Taxonomy. Proceedings of the California Academy of Sciences 56(1): 196–215.

de Queiroz K (2007) Species Concepts and Species Delimitation. Systematic Biology 56(6): 879–886. https://doi.org/10.1080/10635150701701083

Foley S, Krehenwinkel H, Cheng D, Piel WH (2021) Phylogenomic analyses reveal a Gondwanan origin and repeated out of India colonizations into Asia by tarantulas (Araneae: Theraphosidae). PeerJ 9: e11162. https://doi.org/10.7717/peerj.11162

Friedrich M (2013) Biological clocks and visual systems in cave-adapted animals at the dawn of speleogenomics. Integrative and Comparative Biology 53(1): 50–67. https://doi.org/10.1093/icb/ict058

Gibert J, Deharveng L (2002) Subterranean Ecosystems: A Truncated Functional Biodiversity. BioScience 52(6): 473–481. https://doi.org/10.1641/0006-3568(2002)052[0473:SEATFB]2.0.CO:2

Guadanucci JP (2012) Trichobothrial morphology of Theraphosidae and Barychelidae spiders (Araneae, Mygalomorphae). Zootaxa 3439: 1–42. https://doi.org/10.11646/zootaxa.3439.1.1

Guadanucci JPL, Galleti-Lima A, Indicatti RP (2020) Cuticular Structures of New World Tarantulas: Ultramorphology of Setae and Other Features. In: Pérez-Miles F (Ed.) New World Tarantulas. Zoological Monographs 6, Springer Cham, 319–340. https://doi.org/10.1007/978-3-030-48644-0_11

Hamilton CA, Hendrixson BE, Bond JE (2016) Taxonomic revision of the tarantula genus *Aphonopelma* Pocock, 1901 (Araneae, Mygalomorphae, Theraphosidae) within the United States. ZooKeys 560: 1–340. https://doi.org/10.3897/zookeys.560.6264

Hervant F, Malard F (2019) Adaptations: Low Oxygen. In: Encyclopedia of Caves; Elsevier BV: Amsterdam, The Netherlands, 8–15. https://doi.org/10.1016/B978-0-12-814124-3.00002-9

Hirst AS (1909) On some new or little-known mygalomorph spiders from the Oriental region and Australasia. Records of the Indian Museum Calcutta 3(4): 383–390. https://doi.org/10.26515/rzsi/v3/i4/1909/163298

Howarth FG (1980) The zoogeography of specialized cave animals: a bioclimatic model. Evolution 34: 394–406. https://doi.org/10.2307/2407402

Howarth FG (1983) Ecology of Cave Arthropods. Annual Review of Entomology 28: 365–389. https://doi.org/10.1146/annurev.en.28.010183.002053

Howarth FG (2022) Why the delay in recognizing terrestrial obligate cave species in the tropics? International Journal of Speleology 52(1): 23–43. https://doi.org/10.5038/1827-806X.52.1.2446

Husana DE, Naruse T, Kase T (2009) Two new cavernicolous species of the genus *Sundathelphusa* from Western Samar, Philippines (Decapoda: Brachyura: Parathelphusidae). Journal of Crustacean Biology 29: 419–427. https://doi.org/10.1651/08-3081.1

Huson DH, Bryant D (2006) Application of phylogenetic networks in evolutionary studies. Molecular Biology and Evolution 23(2): 254–267. https://doi.org/10.1093/molbev/msj030

Huson DH, Bryant D (2024) The SplitsTree App: interactive analysis and visualization using phylogenetic trees and networks. Nature Methods 21: 1773–1774. https://doi.org/10.1038/s41592-024-02406-3

Jenner RA (2004) The scientific status of metazoan cladistics: why current practice must change. Zoologica Scripta 33: 293–310.

Juan C, Guzik MT, Jaume D, Coopers SJB (2010) Evolution in caves: Darwin's 'wrecks of ancient life' in the molecular era. Molecular Ecology 19(18) 3865–3880. https://doi.org/10.1111/j.1365-294X.2010.04759.x

Koyama T, Mirth CK (2018) Unraveling the diversity of mechanisms through which nutrition regulates body size in insects. Current Opinion in Insect Science 25: 1–8. https://doi.org/10.1016/j.cois.2017.11.002

Li F, Shao L, Li S (2020) Tropical Niche Conservatism Explains the Eocene Migration from India to Southeast Asia in Ochyroceratid Spiders. Systematic Biology 69(5): 987–998. https://doi.org/10.1093/sysbio/syaa006

Lindenmayer D, Scheele B (2017) Do not publish. Science 356(6340): 800–801. https://doi.org/10.1126/science.aan136

Lourenco WR, Rossi A (2019) The cave population of *Chaerilus* Simon, 1877 from Palawan, Philippines, and description of a new species (Scorpiones: Chaerilidae). Comptes Rendus Biologies 342 (1–2): 45–53. https://doi.org/10.1016/j.crvi.2018.12.001

Lucañas CC, Lit Jr IL (2016) Cockroaches (Insecta, Blattodea) from caves of Polillo Island (Philippines), with description of a new species. Subterranean Biology 19: 51–64. https://doi.org/10.3897/subtbiol.19.9804

Mammola S, Isaia M (2017) Spiders in caves. Proceedings of the Royal Society B Biological Sciences 284(20170193): 1–10. https://doi.org/10.1098/rspb.2017.0193

Mendoza MJI (2014) Taxonomic revision of *Hemirrhagus* Simon, 1903 (Araneae: Theraphosidae, Theraphosinae), with description of five new species from Mexico. Zoological Journal of the Linnean Society 170: 634–689. https://doi.org/10.1111/zoj.12112

Mendoza JI, Francke OF (2018) Five new cave-dwelling species of *Hemirrhagus* Simon 1903 (Araneae, Theraphosidae, Theraphosinae), with notes on the generic distribution and novel morphological features. Zootaxa 4407(4): 451–482. https://doi.org/10.11646/zootaxa.4407.4.1

Midgley JM, Engelbrecht I (2019) New collection records for Theraphosidae (Araneae, Mygalomorphae) in Angola, with the description of a remarkable new species of Ceratogyrus. African Invertebrates 60(1): 1–13. https://doi.org/10.3897/AfrInvertebr.60.32141.

Morgan K, Linton YM, Somboon P, Saikia P, Dev V, Socheat D, Walton C (2010) Inter-specific gene flow dynamics during the Pleistocene-dated speciation of forest-dependent mosquitoes in Southeast Asia. Molecular Ecology 19(11): 2269–85. https://doi.org/10.1111/j.1365-294X.2010.04635.x

Nei M, Kumar S (2000) Molecular Evolution and Phylogenetics. Oxford University Press, New York. https://doi.org/10.1093/oso/9780195135848.001.0001

Nunn S, West R, Wirth V (2016) A revision of the selenocosmiine tarantula genus *Phlogiellus* Pocock 1897 (Araneae: Theraphosidae), with description of 4 new species. International Journal of Zoology 2016(9895234): 1–54. https://doi.org/10.1155/2016/9895234

Ortega-Escobar J, Ruiz MA (2017) Role of the different eyes in the visual odometry in the wolf spider Lycosa tarantula (Araneae, Lycosidae). Journal of Experimental Biology 220(2): 259–265. https://doi.org//10.1242/jeb.145763

Ortiz D, Francke OF, Bond JE (2018) A tangle of forms and phylogeny: Extensive morphological homoplasy and molecular clock heterogeneity in *Bonnetina* and related tarantulas. Molecular Phylogenetics and Evolution 127: 55–73. https://doi.org/10.1016/j.ympev.2018.05.013

Palmer A (1991) Origin and morphology of limestone caves. Geological Society of America Bulletin 103(1): 1–21. https://doi.org/10.1130/0016-7606(1991)103%3C0001:OAMOLC%3E2.3.CO;2

Partha R, Chauhan BK, Ferreira Z, Robinson JD, Lathrop K, Nischal KK, Chikina M, Clark NL (2017) Subterranean mammals show convergent regression in ocular genes and enhancers, along with adaptation to tunneling. eLife 6: e25884. https://doi.org/10.7554/eLife.25884

Poulson TL, White WB (1969) The cave environment. Science 165: 971–981. https://doi.org/10.1126/science.165.3897.971

Posada D, Crandall KA (2001) Intraspecific gene genealogies: Trees grafting into networks. Trends in Ecology & Evolution 16(1): 37–45. https://doi.org/10.1016/S0169-5347(00)02026-7

Raven RJ (1985) The spider infraorder Mygalomorphae (Araneae): cladistics and systematics. Bulletin of the American Museum of Natural History 182: 1–180.

Raven RJ (2005) A new tarantula species from northern Australia (Araneae, Theraphosidae). Zootaxa 1004: 15–28. https://doi.org/10.11646/zootaxa.1004.1.2

Rebora M, Salerno G, Piersanti S (2019) Aquatic Insect Sensilla: Morphology and Function. In: Del-Claro K, Guillermo R (Eds) Aquatic Insects. Springer, Cham, 139–166. https://doi.org/10.1007/978-3-030-16327-3_7

Reissland A, Görner P (1985) Trichobothria. In: Barth FG (Ed.) Neurobiology of Arachnids. Springer, Berlin, Heidelberg, 138–161. https://doi.org/10.1007/978-3-642-70348-5_8

Restificar SDF, Day MJ, Urich PB (2006) Protection of Karst in the Philippines. Acta Carsologica 35(1):121–130. https://doi.org/10.3986/ac.v35i1.248

Romero Jr A (2009) Cave Biology: Life in Darkness. Cambridge University Press. https://doi.org/10.1017/CBO9780511596841

Rouch R, Danielpol D (1987) L'origine de la fauneaquatique souterraine, entre le paradigme durefuge et le mode`le de la colonisation active. Stygologia 3: 345–372.

Salamanes J, Santos J, Austria E, Villancio G (2022) A new species of tarantula of the genus *Orphnaecus* Simon, 1892 (Araneae: Theraphosidae) from the Province of Dinagat Islands, Philippines. Biodiversitas Journal of Biological Diversity 23(8): 4283–4288. https://doi.org/10.13057/biodiv/d230852.

Sereno PC (2009) Comparative cladistics. Cladistics 25: 624–659. https://doi.org/10.1111/j.1096-0031.2009.00265.x

Sharma PP, Baker CM, Cosgrove JG, Johnson JE, Oberski JT, Raven RJ, Harvey MS, Boyer SL, Giribet G (2018) A revised dated phylogeny of scorpions: Phylogenomic support for ancient divergence of the temperate Gondwanan family Bothriuridae. Molecular Phylogenetic Evolution 122:37–45. https://doi.org/10.1016/j.ympev.2018.01.003

Sket B (2008) Can we agree on an ecological classification of subterranean animals? Journal of Natural History 42(21–22): 1549-1563.

Simon E (1892) Arachnides. In: Raffrey A, Bolivar I, Simon E (Eds) Etudes cavernicoles de l'île Luzon. Voyage de M. E. Simon aux l'îles Phillipines (mars et avril 1890). 4e Mémoire. Annales de la Société Entomologique de France 61: 35–52. https://doi.org/10.1080/21686351.1892.12279283

Stoch F (2002) Italian habitats. Caves and karstic phenomena: life in subterranean world. Italian Ministry of the Environment and Territory Protection and Friuli Museum of Natural History, Udine, 159 pp.

Tamura K, Battistuzzi FU, Billing-Ross P, Murillo O, Filipski A, Kumar S (2012) Estimating Divergence Times in Large Molecular Phylogenies. Proceedings of the National Academy of Sciences 109: 19333–19338. https://doi.org/10.1073/pnas.1213199109

Tamura K, Qiqing T, Kumar S (2018) Theoretical Foundation of the RelTime Method for Estimating Divergence Times from Variable Evolutionary Rates. Molecular Biology and Evolution 35: 1770–1782. https://doi.org/10.1093/molbev/msy044

Tamura K, Stecher G, Kumar S (2021) MEGA 11: Molecular Evolutionary Genetics Analysis Version 11. Molecular Biology and Evolution 38(7): 3022–3027. https://doi.org/10.1093/molbev/msab120

Trajano E (2012) Ecological Classification of Subterranean Organisms. Encyclopedia of Caves. 275–277. https://doi.org/10.1016/B978-0-12-383832-2.00035-9

West RC, Nunn SC, Hogg S (2012) A new tarantula genus, *Psednocnemis*, from West Malaysia (Araneae: Theraphosidae), with cladistic analyses and biogeography of Selenocosmiinae Simon 1889. Zootaxa 3299: 1–43. https://doi.org/10.11646/zootaxa.3299.1.1

Wirth V, Striffler BF (1995) Neue Erkenntnisse zur Vogelspinnen – Unterfamilie Ornithoctoninae, mit Beschreibung von *Ornithoctonus aureotibialis* sp. n. und *Haplopelma longipes* sp. n. (Araneae, Theraphosidae). Arthropoda 13(2): 2–27.

Wirth V, Hildebrandt K (2023) Preparation techniques of (Bird) spider Spermathecae. British Tarantula Society Journal 2(38): 3–22.

Wunderlich J, Müller P (2020) New and already described fossil spiders (Araneae) of 20 families in mid cretaceous Burmese amber with notes on spider phylogeny, evolution and classification. Beiträge zur Araneologie 13: 22164.

Vandel A (1965) Biospeleology: the biology of cavernicolous animals. Pergamon Press, Oxford, 524 pp. https://doi.org/10.1016/B978-0-08-010242-9.50027-X

Vargovitsh RS (2017) Two new troglobiont *Pygmarrhopalites* species of the *principalis* group (Collembola: Arrhopalitidae) from the West Caucasus. Zootaxa 4250(1): 23–42. https://doi.org/10.11646/zootaxa.4250.1.2